

Multimodal Sparse Bayesian Dictionary Learning

Igor Fedorov

*Department of Electrical and Computer Engineering
University of California, San-Diego
San-Diego, CA 92093, USA*

IFEDOROV@ENG.UCSB.EDU

Bhaskar D. Rao

*Department of Electrical and Computer Engineering
University of California, San-Diego
San-Diego, CA 92093, USA*

BRAO@ENG.UCSB.EDU

Editor:

Abstract

The purpose of this paper is to address the problem of learning dictionaries for multimodal datasets, i.e. datasets collected from multiple data sources. We present an algorithm called multimodal sparse Bayesian dictionary learning (MSBDL). The MSBDL algorithm is able to leverage information from all available data modalities through a joint sparsity constraint on each modality's sparse codes without restricting the coefficients themselves to be equal. Our framework offers a considerable amount of flexibility to practitioners and addresses many of the shortcomings of existing multimodal dictionary learning approaches. Unlike existing approaches, MSBDL allows the dictionaries for each data modality to have different cardinality. In addition, MSBDL can be used in numerous scenarios, from small datasets to extensive datasets with large dimensionality. MSBDL can also be used in supervised settings and allows for learning multimodal dictionaries concurrently with classifiers for each modality.

Keywords: Multimodal, dictionary learning, Bayesian learning

1. Introduction

Due to improvements in sensor technology, acquiring vast amounts of data has become relatively easy. Given the ability to harvest data, the task becomes how to extract relevant information from the data. In most cases, the data is multimodal, which introduces novel challenges in learning from it. Multimodal dictionary learning and sparse coding have become popular tools for fusing multimodal information (Cha et al., 2015; Shekhar et al., 2014; Caicedo and González, 2012; Ding and Rao, 2015; Fedorov et al., 2017).

Let L and J denote the number of data points for each modality and number of modalities, respectively. Let $Y_j = [y_j^1 \ \cdots \ y_j^L] \in \mathbb{R}^{N_j \times L}$ denote the data matrix for modality j , where y_j^i denotes the i 'th data point for modality j . Unless otherwise specified, we use uppercase symbols to denote matrices. The multimodal dictionary learning problem consists of estimating dictionaries $D_j \in \mathbb{R}^{N_j \times M_j}$ and encodings X_j given data Y_j such that

$$Y_j \approx D_j X_j \quad \forall j. \tag{1}$$

We focus on overcomplete dictionaries because they are more flexible in the range of signals they can represent (Donoho et al., 2006). Since y_j^i admits an infinite number of representations under overcomplete D_j , we regularize the solution by constraining x_j^i to be sparse (Aharon et al., 2006a).

Without any further constraints, the multimodal dictionary learning problem can be viewed as J independent unimodal problems. To fully capture the multimodal nature of the problem, the learning process must be adapted to encode the prior knowledge that each set of points $\{y_j^i\}_{j=1}^J$ is generated by a common source which is measured J different ways. For instance, in (Yang et al., 2010), low and high resolution image patches are modelled as y_1^i and y_2^i , respectively, and the association between y_1^i and y_2^i is enforced by the constraint $x_1^i = x_2^i$. The resulting multimodal dictionary learning problem, referred to here as ℓ_1 DL, is to solve (Mairal et al., 2009)

$$\arg \min_{\tilde{D}, X} \left\| \tilde{Y} - \tilde{D}X \right\|_F^2 + \lambda \|X\|_1 \quad (2)$$

$$\tilde{Y} = \begin{bmatrix} Y_1 \\ \vdots \\ Y_J \end{bmatrix}, \quad \tilde{D} = \begin{bmatrix} D_1 \\ \vdots \\ D_J \end{bmatrix} \quad (3)$$

where $\|\cdot\|_F$ denotes the Frobenius norm, $\|X\|_1 = \sum_{i=1}^L \|x^i\|_1$, and the ℓ_1 -norm is used as a convex proxy to the ℓ_0 sparsity measure. In a classification framework, (2) can be viewed as learning a multimodal feature extractor, where the optimizer is the multimodal representation of $\{y_j^i\}_{j=1}^J$ that is fed into a classifier (Cha et al., 2015; Gwon et al., 2015; Shekhar et al., 2014). There are four significant deficiencies associated with using ℓ_1 DL for multimodal dictionary learning:

- D1** While using the same sparse code for each modality establishes an explicit relationship between the dictionaries for each modality, the same coefficient values may not be able to represent different modalities well.
- D2** Some data modalities are often less noisy than others and the algorithm should be able to leverage the clean modalities to learn on the noisy ones. Since (2) constrains λ to be the same for all modalities, it is unclear how the learning algorithm can incorporate prior knowledge about the noise level of each modality.
- D3** The formulation in (2) constrains $M_j = M \forall j$, for some M . Since some modalities can have drastically different dimensionality than others, it is desirable to allow M_j to vary.
- D4** The choice of λ is central to the success of approaches like (2). If λ is chosen too high, the reconstruction term is ignored completely, leading to poor dictionary quality. If λ is chosen too low, the sparsity promoting term is effectively eliminated from the objective function. Extensive work has been done to approach this hyperparameter selection problem from various angles. Two popular approaches include treating the hyperparameter selection problem as an optimization problem of its own (Bergstra and Bengio, 2012; Bergstra et al., 2011) and grid search, with the latter being the prevailing strategy in the dictionary learning community (Mairal et al., 2009;

Jiang et al., 2013). In either case, optimization of λ usually involves evaluating (2) at various choices of λ , which can be computationally intensive and lead to suboptimal results in practice.

1.1 Related Work

In the following, we review several relevant works from the dictionary learning literature. For each method, we highlight its benefits and drawbacks in light of **D1-D4**.

One of the seminal unimodal dictionary learning algorithms is K-SVD, which seeks to solve (Aharon et al., 2006a)

$$\min_{D, \{\|x^i\|_0 \leq s\}_{i=1}^L} \|Y - DX\|_F^2 \quad (4)$$

where s denotes the desired sparsity level and modality subscripts have been omitted since $J = 1$ in the unimodal scenario. The K-SVD algorithm proceeds in a block-coordinate descent fashion, where D is optimized while holding X fixed and vice-versa. The update of X involves a greedy ℓ_0 pseudo-norm minimization procedure called Orthogonal Matching Pursuit (Pati et al., 1993). In a multimodal setting, K-SVD can be naively adapted, where Y is replaced by \tilde{Y} and D by \tilde{D} in (4), as in (2).

One recent approach, referred to here as Joint ℓ_0 Dictionary Learning ($J\ell_0$ DL), builds upon K-SVD for the multimodal dictionary learning problem and proposes to solve (Ding and Rao, 2015)

$$\arg \min_{\{\{\chi_j^i = \chi^i\}_{j=1}^J, |\chi^i| \leq s\}_{i=1}^L} \sum_{j=1}^J \lambda_j \|Y_j - D_j X_j\|_F^2 \quad (5)$$

where χ_j^i denotes the support of x_j^i . The $J\ell_0$ DL algorithm tackles **D1-D2** by establishing a correspondence between the supports of the sparse codes for each modality and by allowing modality specific regularization parameters, which allow for encoding prior information about the noise level of y_j^i . On the other hand, $J\ell_0$ DL does not address **D3** and presents even more of a challenge than ℓ_1 DL with respect to **D4** since the size of the grid search needed to find $\{\lambda_j\}_{j=1}^J$ grows exponentially with J . Another major drawback of $J\ell_0$ DL is that, since (5) has an ℓ_0 type constraint, solving it requires an algorithm called Distributed Compressive Sensing Simultaneous Orthogonal Matching Pursuit (DCS-SOMP) (Baron et al., 2009). DCS-SOMP is a greedy algorithm and can produce poor solutions, especially if some modalities are much noisier than others.

The multimodal version of (2), referred to here as Joint ℓ_1 DL ($J\ell_1$ DL), seeks (Bahrampour et al., 2016)

$$\arg \min_{\{D_j, X_j\}_{j=1}^J} \frac{1}{2} \sum_{i=1}^L \sum_{j=1}^J \|y_j^i - D_j x_j^i\|_2^2 + \lambda \|\Pi^i\|_{12} \quad (6)$$

where $\Pi^i = [x_1^i \ \cdots \ x_J^i]$ and

$$\|\Pi^i\|_{12} = \sum_{m=1}^M \|\Pi^i[m, :]\|_2, \quad (7)$$

where $\Pi[m, :]$ denotes the m 'th row of Π^i . The ℓ_{12} -norm in (6) promotes row sparsity in Π^i , which promotes $\{x_j^i\}_{j=1}^J$ that share the same support. Like all of the previous approaches, $J\ell_1$ DL adopts a block-coordinate descent approach to solving (6), where an alternating direction method of multipliers algorithm is used to compute the sparse code update stage (Parikh et al., 2014). While $J\ell_1$ DL makes progress toward addressing **D1**, it does so at the cost of sacrificing the hard constraint that $\{x_j^i\}_{j=1}^J$ share the same support. The authors of (Bahrampour et al., 2016) attempt to address **D2** by relaxing the constraint on the support of $\{x_j^i\}_{j=1}^J$ even more, but we will not study this approach here because it moves even further from the theme of this work. In addition, $J\ell_1$ DL does not address **D3-D4**.

One desirable property of dictionary learning approaches is that they be scalable with respect to the size of the dictionary as well as the dataset. When L becomes large, the algorithm must be able to learn in a stochastic manner, where only a subset of the data samples need to be processed at each iteration. Stochastic learning strategies have been studied in the context of ℓ_1 DL (Mairal et al., 2009, 2012) and $J\ell_1$ DL (Bahrampour et al., 2016), but not for K-SVD or $J\ell_0$ DL. Likewise, when N_j becomes large, the computational complexity of the algorithm should not be prohibitive.

When the dictionary learning algorithm is to be used as a building block in a classification framework, it is beneficial to incorporate class information within the learning process itself. In the supervised setting, the input to the algorithm is $\{\{Y_j\}_{j=1}^J, Q\}$, where $Q = [q^1 \ \cdots \ q^L] \in \mathbb{B}^{C \times L}$ is the binary class label matrix for the dataset and C is the number of classes. Each vector q^i is the label for the i 'th data point in a one-of- C format. This type of dictionary learning is referred to as task-driven (Bahrampour et al., 2016; Mairal et al., 2012), label consistent (Jiang et al., 2013), or discriminative (Zhang and Li, 2010) dictionary learning and the goal is to learn a dictionary D_j such that x_j^i is indicative of the label associated with y_j^i . For instance, the discriminative K-SVD (D-KSVD) algorithm seeks to solve (Zhang and Li, 2010)

$$\arg \min_{D, W, \{\|x^i\|_0 \leq s\}_{i=1}^L} \|Y - DX\|_F^2 + \lambda_{su} \|Q - WX\|_F^2 \quad (8)$$

where W can be viewed as a linear classifier for the sparse code matrix X . An extension of D-KSVD, called label consistent K-SVD, appends another term to (8) to promote learning dictionaries where a given dictionary column corresponds to a single class (Jiang et al., 2013). Interestingly, it has recently been shown that there is no benefit to label consistent K-SVD over D-KSVD when the dictionary atoms are uniformly distributed among the classes in the label consistent K-SVD formulation (Kviatkovsky et al., 2017).

The task-driven ℓ_1 DL (TD- ℓ_1 DL) algorithm seeks to solve (Mairal et al., 2012)

$$\arg \min_{D, W} E_x [l_{su}(q, W, x^*(y, D))] + \nu \|W\|_F^2 \quad (9)$$

where $E_x[\cdot]$ denotes the expectation with respect to $p(x)$, $l_{su}(\cdot)$ denotes the supervised loss function¹, $x^*(y, D)$ is shorthand for the solution of (2) with the dictionary fixed to D , and the last term provides regularization on W to avoid over-fitting.

1. Examples of supervised losses include the squared loss in (8), logistic loss, and hinge loss (Mairal et al., 2012).

Likewise, the task-driven $J\ell_1$ DL (TD- $J\ell_1$ DL) algorithm seeks to solve (Bahrampour et al., 2016)

$$\arg \min_{\{D_j, W_j\}_{j=1}^J} E_{\{x_j\}_{j=1}^J} \left[\sum_{j=1}^J l_{su}(q_j, W_j, x_j^*(y_j, D_j)) \right] + \nu \sum_{j=1}^J \|W_j\|_F^2 \quad (10)$$

where $x_j^*(y_j, D_j)$ denotes the sparse code for the j 'th modality in the optimizer of (6) with dictionaries fixed to $\{D_j\}_{j=1}^J$.

1.2 Contributions

In this work, we build upon the multimodal sparse Bayesian dictionary learning algorithm (MSBDL), which we introduced in (Fedorov et al., 2017) to address **D1-D2**. MSBDL is based on a hierarchical sparse Bayesian model, which was introduced in the context of Sparse Bayesian Learning (Girolami, 2001; Tipping, 2001; Wipf and Rao, 2004; Ji et al., 2009; Zhang and Rao, 2011; Ding and Rao, 2015) and has since been extended to various structured learning problems (Fedorov et al., 2016, 2018; Nalci et al., 2016). MSBDL is able to capture the relationship between diverse datasets within the dictionary learning process, while addressing **D1-D2** and benefiting from the significant sparse coding performance gains afforded by the Bayesian model (Giri and Rao, 2016; Ding and Rao, 2015). Here, we extend MSBDL to tackle **D1-D4** as well as scalable and task-driven learning:

1. We extend MSBDL to address **D3**. To the best of our knowledge, this represents the first multimodal dictionary learning algorithm capable of learning differently sized dictionaries.
2. We extend MSBDL to the task-driven learning scenario (TD-MSBDL) and show that closed-form inference comes at negligible additional computational cost.
3. We present scalable versions of MSBDL.
4. We provide an almost hyperparameter free optimization strategy which can be used to apply MSBDL on a novel dataset with minimal tuning. We provide a theoretical analysis of the benefits of the proposed approach.
5. We show that multimodal dictionary learning offers provable advantages compared to unimodal dictionary learning.

2. Proposed Approach

Let $\mathbf{y}_j, \mathbf{x}_j$, and D_j be random variables representing y_j^i, x_j^i , and D_j , respectively². The graphical model for the MSBDL algorithm is shown in Fig. 1. The signal model is given by

$$\mathbf{y}_j = D_j \mathbf{x}_j + \mathbf{v}_j, \quad \mathbf{v}_j \sim \mathcal{N}(\mathbf{v}_j; 0, \sigma_j^2 \mathbf{I}) \quad (11)$$

where $\mathcal{N}(\cdot)$ denotes a Gaussian distribution and the noise variance is allowed to vary among modalities. In order to encourage x_j^i to be sparse, we assume a Gaussian Scale

2. We use bold symbols to indicate random variables.

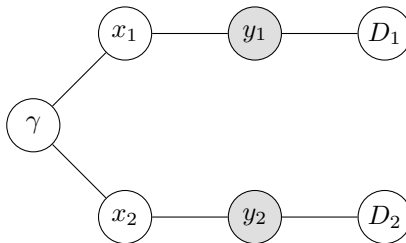


Figure 1: Graphical model for two modality MSBDL.

Mixture (GSM) prior on each element of \mathbf{x}_j (Tipping, 2001; Wipf and Rao, 2004, 2007; Wipf et al., 2011). The GSM prior is a popular class of distributions whose members include many sparsity promoting priors, such as the Laplacian and Student's-t distributions (Tipping, 2001; Wipf and Rao, 2004, 2007; Wipf et al., 2011; Palmer, 2006; Giri and Rao, 2016; Fedorov et al., 2018). The remaining task is to specify the conditional density of \mathbf{x}_j given γ . One option is to use (Fedorov et al., 2017):

$$p(x_j|\gamma) = \prod_{m=1}^M \mathcal{N}(x_j[m]; 0, \gamma[m]) \quad (12)$$

where $x_j[m]$ denotes the m 'th element of the vector x_j and the choice of $p(\gamma[m])$ determines the marginal density of $\mathbf{x}_j[\mathbf{m}]$. We assume a non-informative prior on $\gamma_j[\mathbf{m}]$ (Tipping, 2001). As will be shown in Section 2.2, the conditional distribution in (12) represents a Bayesian realization of the constraint that $\{x_j\}_{j=1}^J$ must share the same support. Since (12) represents a relationship between individual elements of x_j , we refer to (12) as the one-to-one prior.

2.1 Inference Procedure

We adopt an empirical Bayesian inference strategy (MacKay, 1992). Let $\theta = \{\{D_j\}_{j=1}^J, \{\gamma^i\}_{i=1}^L\}$. The goal is to find

$$\arg \max_{\theta} \log p(\{Y_j\}_{j=1}^J | \theta) \quad (13)$$

where

$$p(\{Y_j\}_{j=1}^J | \theta) = \prod_{i=1, j=1}^{L, J} p(y_j^i | \theta) \quad (14)$$

$$p(y_j^i | \theta) = \mathcal{N}(y_j^i; 0, \Sigma_{y,j}^i) \quad (15)$$

$$\Sigma_{y,j}^i = \sigma_j^2 \mathbf{I} + D_j \Gamma^i D_j^T \quad (16)$$

$$\Gamma^i = \text{diag}(\gamma^i). \quad (17)$$

We use the Expectation-Maximization (EM) algorithm to maximize (13), where $\{\{X_j, Y_j\}_{j=1}^J, \theta\}$ and $\{X_j\}_{j=1}^J$ are treated as the complete and nuisance data, respectively.

At iteration t , the E-step computes

$$Q(\theta, \theta^t) = \left\langle \log p \left(\{Y_j, X_j, D_j, \sigma_j\}_{j=1}^J, \{\gamma^i\}_{i=1}^L \right) \right\rangle \quad (18)$$

where $\langle \cdot \rangle$ denotes the expectation with respect to $p \left(\{X_j\}_{j=1}^J \mid \{Y_j\}_{j=1}^J, \theta^t \right)$, and θ^t denotes the estimate of θ at iteration t . Due to the conditional independence properties of the model, the posterior factors over i and

$$p(x_j^i | y_j^i, \theta) = \mathbf{N}(x_j^i; \mu_j^i, \Sigma_{x,j}^i) \quad (19)$$

$$\Sigma_{x,j}^i = \left(\sigma_j^{-2} D_j^T D_j + (\Gamma^i)^{-1} \right)^{-1} \stackrel{a}{=} \Gamma^i - \Gamma^i D_j^T (\sigma_j^2 \mathbf{1} + D_j \Gamma^i D_j^T)^{-1} D_j \Gamma^i \quad (20)$$

$$\mu_j^i = \sigma_j^{-2} \Sigma_{x,j}^i D_j^T y_j^i \quad (21)$$

where step (a) follows from the matrix inversion lemma. In the M-step, $Q(\theta, \theta^t)$ is maximized with respect to θ . In general, the M-step depends on the choice of $p(x_j | \gamma)$. For the choice in (12), the M-step becomes

$$(\gamma^i[m])^{t+1} = \frac{\sum_{j=1}^J \Sigma_{x,j}^i[m, m] + \left(\mu_j^i[m] \right)^2}{J} \quad (22)$$

$$D_j^{t+1} = Y_j U_j^T \left(U_j U_j^T + \sum_{i=1}^L \Sigma_{x,j}^i \right)^{-1}. \quad (23)$$

2.2 How does MSBDL solve deficiency D1?

One consequence of the GSM prior is that many of the elements of γ^i converge to 0 during inference³. When $\gamma^i[m] = 0$, the posterior of $x_j^i[m]$ reduces to $\delta(x_j[m])$ for all j , where $\delta(\cdot)$ denotes the Dirac-delta function (Wipf and Rao, 2004). In other words, the prior in (12) represents a Bayesian realization of the constraint that $\{x_j\}_{j=1}^J$ must share the same support. On the other hand, for $\gamma[m] > 0$, $x_j[m]$ is unconstrained. Therefore, (12) constrains $\{x_j\}_{j=1}^J$ to share the same support while allowing coefficient values to vary between modalities.

2.3 Connection to $\mathbf{J}\ell_1\mathbf{DL}$

Suppose that the conditional distribution in (12) is used with

$$\gamma[\mathbf{m}] \sim \text{Ga} \left(\frac{J}{2}, 1 \right) \quad \forall \mathbf{m} \quad (24)$$

where $\text{Ga}(\cdot)$ refers to the Gamma distribution. It can be shown that (Boisbunon, 2012)

$$p \left(\{x_j^i\}_{j=1}^J \right) = c \prod_{m=1}^M K_0 \left(\left\| [x_1^i[m] \ \cdots \ x_J^i[m]] \right\|_2 \right) \quad (25)$$

3. This has been proven in the context of sparse signal recovery (Wipf and Rao, 2004), i.e. when D_j is known and fixed. Although we observe experimentally that MSBDL converges to sparse solutions, we do not prove that this is guaranteed in general.

where c is a normalization constant and $K_0(\cdot)$ denotes the modified Bessel function of the second kind and order 0. For large x , $K_0(x) \approx \frac{\pi}{\sqrt{2\pi x}} \exp(-x)$ (Eltoft et al., 2006). In the following, we replace $K_0(x)$ by its approximation for purposes of exposition. Under the constraint $\sigma_j = 0.5\lambda \forall j$, the maximum a-posteriori (MAP) estimate of $\{D_j, X_j\}_{j=1}^J$ is given by

$$\arg \min_{\{D_j, X_j\}_{j=1}^J} \frac{1}{2} \sum_{i=1, j=1}^{L, J} \|y_j^i - D_j x_j^i\|_2^2 + \lambda \|\Pi^i\|_{12} + \frac{\lambda}{2} \sum_{i=1, m=1}^{L, M} \log \|\Pi^i[m, :]\|_2. \quad (26)$$

This analysis exposes a number of interesting similarities between the MSBDL and $J\ell_1$ DL models. First, if we ignore the last term in (26), then we find that $J\ell_1$ DL is the MAP estimator of $\{D_j, X_j\}_{j=1}^J$ under the one-to-one prior in the MSBDL model. Second, if we keep the last term in (26), the effect is to add additional regularization on the rows of Π^i in the form of the logarithm of the ℓ_2 norm of each row. Regularizers based on the logarithm function are common in the sparse recovery literature and correspond to a Generalized Double Pareto prior on the signal (Giri and Rao, 2016; Candes et al., 2008).

At the same time, (26) shows that there are significant differences between MSBDL and $J\ell_1$ DL. First, the $J\ell_1$ DL objective function assumes σ_j is constant across modalities, which can lead to a strong mismatch between data and model when the dataset consists of sources with disparate noise levels. Second, in contrast to $J\ell_1$ DL, MSBDL enjoys all of the benefits which evidence maximization offers over MAP estimation (MacKay, 1996, 1992; Giri and Rao, 2016). Evidence maximization naturally embodies "Occam's razor" by penalizing unnecessarily complex models and searches for areas of large mass of the posterior, which are more informative than the mode when the posterior is not well-behaved.

3. Complete Algorithm

So far, it has been assumed that $\{\sigma_j\}_{j=1}^J$ is known. Although it is possible to include $\{\sigma_j\}_{j=1}^J$ in θ and estimate it within the evidence maximization framework in (13), the resulting update rule is known to suffer from an identifiability issue (Wipf and Rao, 2007). An alternative approach is described next. Consider the MAP estimate of x_j given y_j and D_j :

$$\arg \min_{x_j} \|y_j - D_j x_j\|_2^2 - 2\sigma_j^2 \log p(x_j). \quad (27)$$

The estimator in (27) shows that σ_j^2 can be thought of as a regularization parameter which controls the trade-off between sparsity and reconstruction error. As such, we propose to anneal σ_j , favoring increasingly sparse solutions with increasing iteration number. The motivation for annealing σ_j^2 is that the quality of $\{D_j\}_{j=1}^J$ increases with t , so seeking sparse x_j for small t can force EM to converge to a poor stationary point.

Let $\sigma_j^0 > \sigma_j^\infty, \alpha_\sigma < 1$,

$$\tilde{\sigma}_j^{t+1} = \max(\sigma_j^\infty, \alpha_\sigma \sigma_j^t), \quad (28)$$

where σ_j^∞ represents a predefined lowerbound for σ_j and α_σ represents the annealing rate. The proposed annealing strategy can then be stated as

$$\sigma_j^{t+1} = \begin{cases} \tilde{\sigma}_j^{t+1} & \text{if } \log p(Y_j|\theta^t, \tilde{\sigma}_j^{t+1}) > \log p(Y_j|\theta^t, \sigma_j^t) \\ \sigma_j^t & \text{else.} \end{cases} \quad (29)$$

Section 7 studies the motivation for and properties of the annealing strategy in greater detail. In practice, the computation of $p(Y_j|\theta^t, \tilde{\sigma}_j^{t+1})$ is a costly operation because it requires the computation of the sufficient statistics in (16) for all L data points and J modalities. To avoid this, we replace the condition in (29) by instead checking whether decreasing σ_j should increase $p(Y_j|\theta^t, \sigma^t)$. This check is performed by checking the sign of the first derivative of $p(Y_j|\theta^t, \sigma^t)$, such that (29) is replaced by

$$\sigma_j^{t+1} = \begin{cases} \tilde{\sigma}_j^{t+1} & \text{if } \frac{\partial \log p(Y_j|\theta^t, \sigma_j^t)}{\partial \sigma_j} < 0 \\ \sigma_j^t & \text{else.} \end{cases} \quad (30)$$

It can be shown that

$$\frac{\partial \log p(Y_j|\theta^t, \sigma_j^t)}{\partial \sigma_j} = - \sum_{i=1}^L (y_j^i)^T V_j^i (\Lambda_j^i)^{-2} (V_j^i)^T y_j^i + \sum_{n=1}^{N_j} (\Lambda_j[n, n] + \sigma_j^2)^{-1} \quad (31)$$

where $V_j^i \Lambda_j^i (V_j^i)^T$ is the eigen-decomposition of $\Sigma_{y,j}^i$ and $(\Lambda_j^i)^{-2}$ represents a diagonal matrix whose $[n, n]$ 'th entry is $(\Lambda_j^i[n, n])^{-2}$. The advantage of (30) over (29) is that it does not require any new computations⁴.

The complete MSBDL algorithm is summarized in Fig. 2. In practice, at each iteration, the dictionaries $\{D_j\}_{j=1}^J$ are normalized to unit ℓ_2 column norm in order to prevent scaling instabilities.

3.1 Dictionary Cleaning

We adopt the methodology used in (Aharon et al., 2006a) and "clean" the dictionaries $\{D_j\}_{j=1}^J$ every T iterations. Cleaning a dictionary D_j involves removing atoms which are aligned with one or more other atoms in the dictionary and replacing the removed atom with the element of Y_j which has the poorest reconstruction under D_j . In addition, a given atom of D_j is replaced if it does not contribute appreciably to representing Y_j , as measured by the energy of the corresponding row of U_j .

4. Scalable Learning

When L is large, it is impractical to update the sufficient statistics for all data points at each EM iteration. To draw a parallel with stochastic gradient descent (SGD), when the objective

4. In other words, no computations other than the ones which have been carried out to find θ^t need to be done. This stems from the fact that (20) requires the computation of $(\Sigma_{y,j})^{-1}$.

Require: $\{Y_j, \sigma_j^0, \sigma_j^\infty\}_{j=1}^J, \alpha_\sigma$

- 1: **while** $\{\sigma_j\}_{j=1}^J$ not converged **do**
- 2: **while** $\{D_j\}_{j=1}^J$ not converged **do**
- 3: **for** $i \in [L]$ **do**
- 4: Update $\{\Sigma_{x,j}^i\}_{j=1}^J$ using (20)
- 5: Update $\{\mu_j^i\}_{j=1}^J$ using (20)
- 6: Update γ^i using (22)
- 7: **end for**
- 8: { Update D_j using (23) if σ_j not converged } $_{j=1}^J$
- 9: **end while**
- 10: { Update σ_j using (30) if σ_j not converged } $_{j=1}^J$
- 11: **end while**
- 12: **return** $\{D_j\}_{j=1}^J$

Figure 2: MSBDL algorithm for the one-to-one prior in (12), where $[L]$ denotes the set $\{1, \dots, L\}$.

function is a sum of functions of individual data points, one can traverse the gradient with respect to a randomly chosen data point at each iteration instead of computing the gradient with respect to every sample in the dataset. In the dictionary learning community, SGD is often the optimization algorithm of choice because the objective function is separable over each data point (Mairal et al., 2009, 2012; Bahrampour et al., 2016).

In addition, as the dimensionality of the data grows, the computation of the sufficient statistics in (20) can become intractable. In the following, we propose to address these issues using a variety of modifications of the MSBDL algorithm from Section 2. The proposed methods also apply to priors on $\{\gamma_j\}_{j=1}^J$ other than the one in (12)⁵.

4.1 Scalability with respect to the size of the dataset

In the following, we review two alternatives to the EM MSBDL algorithm to achieve scalability with respect to L .

4.1.1 BATCH EM

One proposed approach, referred to here as Batch EM, involves computing sufficient statistics only for a randomly chosen subset $\phi = \{i^1, \dots, i^{L_0}\}$ at each EM iteration, where L_0 denotes the batch size. The M-step consists of updating $\{\gamma^i\}_{i \in \phi}$ using (22) and updating D_j using (23), with the exception that only the sufficient statistics from $i \in \phi$ are employed.

4.1.2 INCREMENTAL EM

One stochastic inference alternative is called Incremental EM, which we review next for the case of $J = 1$, omitting modality subscripts for brevity (Neal and Hinton, 1998). Let

5. See Section 5

$F(\tilde{p}, \theta)$ be defined by

$$F(\tilde{p}, \theta) = E_{\tilde{p}} [\log p(X, Y, \theta)] + H(\tilde{p}) \quad (32)$$

where $H(\tilde{p})$ is the entropy of $\tilde{p}(\cdot)$. It can be shown that $p(X|Y, \theta)$ is the unique maximizer of $F(\tilde{p}, \theta)$, given θ . It can also be shown that $F(\tilde{p}, \theta) = \log p(Y|\theta)$ for $\tilde{p}(X) = p(X|Y, \theta)$. It then follows that the E and M steps of EM can be re-stated in the following form:

$$\tilde{p}^{t+1} = \arg \max_{\tilde{p}} F(\tilde{p}, \theta^t) \quad (33)$$

$$\theta^{t+1} = \arg \max_{\theta} F(\tilde{p}^{t+1}, \theta). \quad (34)$$

When the posterior factors over the data points in the dataset, it is reasonable to consider only distributions of the form $\tilde{p}(X) = \prod_{i=1}^L \tilde{p}^i(x^i)$ in (33). Although the factorization constraint may seem restrictive, it should be noted that the maximizer of $F(\tilde{p}, \theta)$ must also factor ⁶ (Neal and Hinton, 1998). It then follows that $F(\tilde{p}, \theta^t) = \sum_{i=1}^L F^i(\tilde{p}^i, \theta^t)$. This leads to a class of algorithms which perform the E-step in an incremental fashion by modifying (33) to

$$(\tilde{p}^i)^{t+1} = \begin{cases} \arg \max_{\tilde{p}^i} F^i(\tilde{p}^i, \theta^t) & \text{if } i \in \phi \\ (\tilde{p}^i)^t & \text{else.} \end{cases} \quad (35)$$

Applying the methodology in (35) and (34) to MSBDL leads to an inference procedure which, at each iteration, randomly selects a subset ϕ of points and updates the sufficient statistics in (20)-(21) for $i \in \phi$. During the M-step, the hyperparameters $\{\gamma^i\}_{i \in \phi}$ are updated. The dictionary D is updated using (23), where the update rule depends on sufficient statistics computed for all L data points, only a subset of which have been updated during the given iteration.

4.2 Scalability with respect to the size of the dictionary

In order to avoid the inversion of the $N_j \times N_j$ matrix required to compute (20), we use the conjugate gradient algorithm to compute μ_j and approximate $\Sigma_{x,j}^i$ by

$$\Sigma_{x,j}^i \approx \left(\text{diag} \left(\sigma^{-2} D_j^T D_j + (\Gamma^i)^{-1} \right) \right)^{-1} \quad (36)$$

where, in this case, $\text{diag}(\cdot)$ denotes setting the off-diagonal elements of the input to 0 (Babacan et al., 2011; Marnissi et al., 2017).

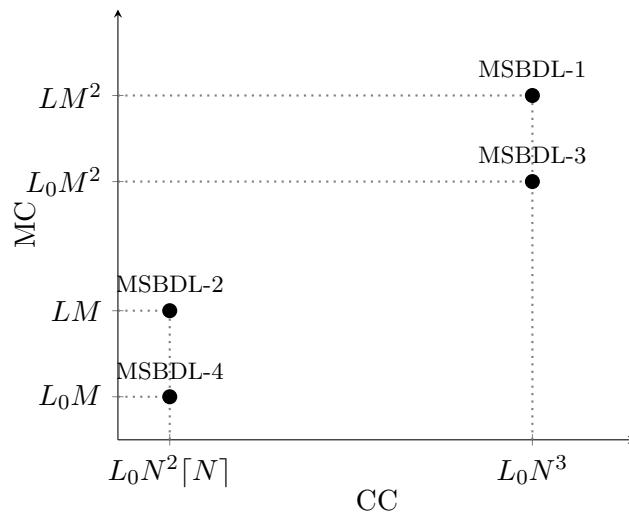
4.2.1 SUMMARY

Table 3a shows a taxonomy of MSBDL algorithms considered using exact or incremental EM and exact or approximate computation of (20)-(21), along with the corresponding worst case computational and memory complexity per EM iteration. Fig. 3b provides a visualization of the difference between the proposed algorithms.

6. In other words, if $\{p^*, \theta^*\}$ is the maximizer of $F(\cdot, \cdot)$, then p^* factors.

	EM Type	μ/Σ_x	CC	MC
MSBDL	Exact	Exact	LN^3	LM^2
MSBDL-1	Incremental	Exact	L_0N^3	LM^2
MSBDL-2	Incremental	Approximate	$L_0N^2\lceil N \rceil$	LM
MSBDL-3	Batch	Exact	L_0N^3	L_0M^2
MSBDL-4	Batch	Approximate	$L_0N^2\lceil N \rceil$	L_0M

(a)



(b)

Figure 3: (3a) Taxonomy of approaches. CC and MC denote worst case computational and memory complexity, respectively. The batch size is denoted by L_0 and $\lceil N \rceil$ denotes a quantity which is upperbounded by d . (3b) Visualization of worst-case computational and memory complexity per modality and EM iteration of the proposed approaches.

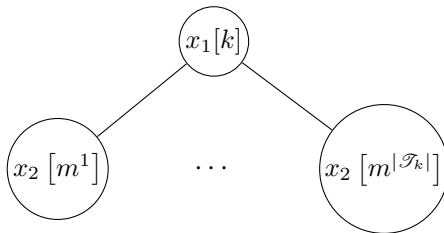


Figure 4

5. Modeling More Complex Relationships

The drawback of the one-to-one prior in (12) is that, like all of the methods surveyed in Section 1, it constrains $\{M_j = M\}_{j=1}^J$. In the following, we propose two models which allow for M_j to be modality-dependent. For ease of exposition, we set $J = 2$, but the models we describe can be readily expanded to $J > 2$. We propose to organize $\{x_j\}_{j=1}^J$ into a tree with K disjoint branches. We adopt the convention that the elements of x_1 form the roots and the elements of x_2 form the leaves of the tree⁷. The root of the k 'th branch is $x_1[k]$ and the leaves are indexed by $\mathcal{T}^k \subseteq [M_2]$, where $[M_2]$ denotes the set $\{1, \dots, M_2\}$. A prototype branch is displayed in Fig. 4.

The defining property of the models we propose is the relationship between the sparsity pattern of the root and leaf levels. As will be shown, the proposed models lend themselves to closed-form EM inference, as in Section 2.1.

5.1 Atom-to-subspace sparsity

The one-to-one prior in (12) can be viewed as linking the one-dimensional subspaces $\{d_j^m\}_{j=1}^2$. Whenever d_1^m is used to represent y_1 , d_2^m must be used to represent y_2 , and vice-versa. The extension to the multi-dimensional subspace case stipulates that if d_1^k is used to represent y_1 , then $\{d_2^m\}_{m \in \mathcal{T}^k}$ must be used to represent y_2 , and vice-versa. It is important to recognize that this model does not constrain $|\mathcal{T}^k|$ to be the same for all k . As a result, M_2 can be chosen completely independently of M_1 ⁸.

Let $\gamma_B \in \mathbb{R}_+^K$. We encode the atom-to-subspace sparsity prior by assigning a single hyperparameter $\gamma_B[k]$ to each subtree k . The conditional distribution for $\{x_j\}_{j=1}^J$ given γ_B is then given by

$$p\left(\{x_j\}_{j=1}^J \mid \gamma_B\right) = \prod_{k=1}^K \mathbf{N}(x_1[k]; 0, \gamma_B[k]) \prod_{m \in \mathcal{T}^k} \mathbf{N}(x_2[m]; 0, \gamma_B[k]). \quad (37)$$

The marginal prior on $\{x_j\}_{j=1}^J$ under $\gamma_B[k] \sim \text{IGa}(\tau/2, \tau/2)$ then takes the form:

$$p\left(\{x_j\}_{j=1}^J\right) = \prod_{k=1}^K ST\left(\left\| \begin{bmatrix} x_1[k] & x_2[\mathcal{T}^k] \end{bmatrix} \right\|_2^2; \tau\right) \quad (38)$$

7. We adopt this convention without loss of generality since the modalities can be re-labeled arbitrarily.

8. Said another way, if $|\mathcal{T}^k| = c \forall k$, then $M_1 = cM_2$.

where $x_2[\mathcal{T}^k]$ is shorthand for the the elements of x_2 indexed by \mathcal{T}^k and $ST(\cdot)$ denotes the Student's-t distribution.

Inference for the prior in (37) proceeds in much the same way as in Section 2.1. The form of the marginal likelihood in (14) and posterior in (19) remain the same, with the exception that $\Sigma_{y,j}^i$ and $\Sigma_{x,j}^i$ are re-defined to be

$$\Sigma_{y,j}^i = \sigma_j^2 \mathbf{1} + D_j \Gamma_j^i D_j^T \quad (39)$$

$$\Sigma_{x,j}^i = \left(\sigma_j^{-2} D_j^T D_j + (\Gamma_j^i)^{-1} \right)^{-1} \quad (40)$$

where $\Gamma_1^i = \text{diag}(\gamma_B^i)$ and Γ_2^i is a diagonal matrix whose $[m, m]$ 'th entry is $\gamma_B^i[k]$ for $m \in \mathcal{T}^k$. The update of γ_B^i is given by

$$(\gamma_B^i[k])^{t+1} = \frac{\Sigma_{x,1}^i[m, m] + (\mu_1^i[m])^2 + \sum_{m \in \mathcal{T}^k} \Sigma_{x,2}^i[m, m] + (\mu_2^i[m])^2}{1 + |\mathcal{T}^k|}, \quad (41)$$

while the update of D_j remains identical to (23).

While the prior in (38) achieves the desired result of allowing for M_j to vary across modalities, it has some limitations. One problem is that, for $|\mathcal{T}^k| > 1$, the atoms of D_2 indexed by \mathcal{T}^k are not identifiable. The reason for the identifiability issue is that D_2 appears in the objective function in (14) only through the $D_2 \Gamma_2 D_2^T$ term in (39), which can be written as

$$D_2 \Gamma_2 D_2^T = \sum_{k=1}^K \gamma_B[k] \sum_{m \in \mathcal{T}^k} d_2^m (d_2^m)^T. \quad (42)$$

Therefore, any D_2' which satisfies $\sum_{m \in \mathcal{T}^k} d_2'^m (d_2'^m)^T = \sum_{m \in \mathcal{T}^k} d_2^m (d_2^m)^T$ for all k achieves the same objective function value as D_2 . Since the objective function is agnostic to the individual atoms of D_2 , the performance of this model is severely upper-bounded in terms of the ability to recover D_2 . In the following, we propose an alternative model which circumvents the identifiability problem.

5.2 Hierarchical Sparsity

In this section, we propose a model which allows the root of each tree branch to control the sparsity of the leaves, but not vice-versa. Specifically, we stipulate that if $x_1[k] = 0$, then $x_2[m] = 0 \forall m \in \mathcal{T}^k$. Hierarchical sparsity was first studied in (Kim and Xing, 2010; Jenatton et al., 2011; Zhao et al., 2009) and later incorporated into a unimodal dictionary learning framework in (Jenatton et al., 2010). Later, Bayesian hierarchical sparse signal recovery techniques were developed, which form the basis for the following derivation (Zhang et al., 2014; Zhang and Kingsbury, 2013).

From an optimization point of view, hierarchical sparsity can be promoted through a cleverly defined composite regularizer (Zhao et al., 2009). In the case of Fig. 4, the regularizer could⁹ take the form

$$\sum_{k=1}^K \sum_{m \in \mathcal{T}^k} \left\| \begin{bmatrix} x_1[k] & x_2[m] \end{bmatrix} \right\|_2 + |x_2[m]|. \quad (43)$$

9. The exact form of the regularizer depends on how the energy in a given group is measured.

As described in (Zhao et al., 2009), the key to designing a composite regularizer for a given root-leaf pair is to measure the group norm of the pair along with the energy of the leaf alone. The combination of the group and individual norms serve two purposes which, jointly, promote hierarchical sparsity (Zhao et al., 2009):

1. it is possible that $x_2[m] = 0, m \in \mathcal{T}^k$, without requiring $x_1[k] = 0$, and
2. the infinitesimal penalty on $x_1[k]$ deviating from 0 tends to 0 for $|x_2[m]| > 0, m \in \mathcal{T}^k$.

In a Bayesian setting, we can mimic the effect of the regularizer in (43) through an appropriately defined prior on $\{\mathbf{x}_j\}_{j=1}^J$. Let

$$\tilde{x}_j = S_j x_j, \quad S_1 \in \mathbb{B}^{M_2 \times M_1}, \quad S_2 = [\mathbf{1} \quad \mathbf{1}]^T \in \mathbb{B}^{2M_2 \times M_1} \quad (44)$$

where S_1 is a binary matrix such that $S_1[m, k] = 1$ if and only if $m \in \mathcal{T}^k$. Let R_j be a diagonal matrix such that $S_j^T S_j R_j = \mathbf{1}^{10}$ and define $\hat{x}_j = S_j R_j x_j$. Let $\gamma_j \in \mathbb{R}^{M_2} \forall j$ and the conditional prior on $\{\mathbf{x}_j\}_{j=1}^J$ given $\{\gamma_j\}_{j=1}^J$ be

$$p\left(\{x_j\}_{j=1}^J \mid \{\gamma_j\}_{j=1}^J\right) = \mathbf{N}(\hat{x}_1; 0, \Gamma_1) \mathbf{N}(\hat{x}_2; 0, \Gamma_2) \quad (45)$$

where $\Gamma_1 = \text{diag}(\gamma_1)$ and $\Gamma_2 = \text{diag}\left([\gamma_1^T \quad \gamma_2^T]^T\right)$. Marginalizing over $\{\gamma_j\}_{j=1}^J$ for $\gamma_j[\mathbf{m}] \sim \text{IGa}(\tau/2, \tau/2)$, the prior on $\{\mathbf{x}_j\}_{j=1}^J$ turns out to be

$$p\left(\{x_j\}_{j=1}^J\right) = \prod_{k=1}^K \prod_{m \in \mathcal{T}^k} ST\left(\| [x_1[k] \quad x_2[m]] \|_2^2; \tau\right) ST\left(x_2[m]^2; \tau\right). \quad (46)$$

Inference for the tree-structured model proceeds in a similar fashion to that shown in Section 2.1, with a few variations. The goal is to optimize (13) through the EM algorithm. The difference here is that we use $\left\{\left\{\hat{X}_j, Y_j\right\}_{j=1}^J, \theta\right\}$ and $\left\{\hat{X}_j\right\}_{j=1}^J$ as the complete and nuisance data, respectively. In order to carry out EM inference, we must first find the posterior density $p\left(\left\{\hat{X}_j\right\}_{j=1}^J \mid \left\{Y_j\right\}_{j=1}^J, \theta\right)$. To find the posterior, it is first helpful to derive the signal model in terms of $\{\hat{x}_j\}_{j=1}^J$, which is given by (Zhang et al., 2014)

$$p(y_j | A_j, \hat{x}_j, \sigma_j) = \mathbf{N}(y_j; A_j S_j^T \hat{x}_j, \sigma_j^2 \mathbf{1}). \quad (47)$$

Using (47), it is straightforward to show that the posterior is given by

$$p(\hat{x}_j^i | y_j^i, \theta) = \mathbf{N}(\hat{x}_j^i; \mu_{\hat{x}, j}^i, \Sigma_{\hat{x}, j}^i) \quad (48)$$

$$\Sigma_{\hat{x}, j}^i = \left(\sigma_j^{-2} S_j D_j^T D_j S_j^T + (\Gamma_j^i)^{-1}\right)^{-1} \quad (49)$$

$$\mu_{\hat{x}, j}^i = \sigma_j^{-2} \Sigma_{\hat{x}, j}^i D_j S_j^T y_j. \quad (50)$$

10. A diagonal R_j is guaranteed to exist because $S_j^T S_j$ is itself a diagonal matrix.

Note that the likelihood function itself is different from that shown in (14)-(16) and is given by

$$p(y_j^i|\theta) = \mathbf{N}(y_j^i; 0, \Sigma_{\hat{y},j}^i) \quad (51)$$

$$\Sigma_{\hat{y},j}^i = \sigma_j^2 \mathbf{1} + D_j S_j^T \Gamma_j^i S_j D_j^T. \quad (52)$$

The update rules are given by¹¹

$$(\gamma_j^i[m])^{t+1} = \begin{cases} 0.5 \sum_{j'=1}^2 \Sigma_{\hat{x},j'}^i[m, m] + (\mu_{\hat{x},j'}^i[m])^2 & \text{if } m \leq M_2 \\ \Sigma_{\hat{x},j}^i[m, m] + (\mu_{\hat{x},j}^i[m])^2 & \text{else.} \end{cases} \quad (53)$$

$$(D_j)^{t+1} = Y_j U_j^T S_j \left(S_j^T \left(U_j U_j^T + \sum_{i=1}^L \Sigma_{\hat{x},j}^i \right) S_j \right)^{-1} \quad (54)$$

5.3 Avoiding Poor Stationary Points

For both the atom-to-subspace and hierarchical sparsity models, we experimentally observe that MSBDL tends to get stuck in undesirable stationary points. In the following, we describe the behavior of MSBDL in these situations and offer a solution.

Suppose that data is generated according to the atom-to-subspace model, where D_j denotes the true dictionary for modality j . In this scenario, we experimentally observe that MSBDL performs well when $|\mathcal{T}^k| = c \forall k$. On the other hand, if $|\mathcal{T}^k|$ varies as a function of k , MSBDL tends to get stuck in poor stationary points, where the quality of a stationary point is (loosely) defined next. Let $|\mathcal{T}^k| = 1$ for all k except k' , for which $|\mathcal{T}^{k'}| = 2$, i.e. $M_2 = M_1 + 1$. In this case, MSBDL is able to recover D_1 , but recovers only the atoms of D_2 which are indexed by $\mathcal{T}^k \forall k \neq k'$.

To avoid the problem of poor stationary points, we adopt the following strategy. If the tree describing the assignment of columns of D_2 to those of D_1 is unbalanced, i.e. $|\mathcal{T}^k|$ varies with k , then we first balance the tree¹² by adding additional leaves. Let \hat{M}_2 be the number of leaves in the balanced tree. We run the MSBDL algorithm until convergence to generate $\{\hat{D}_j\}_{j=1}^J$. Finally, we prune away $\hat{M}_2 - M_2$ columns of \hat{D}_2 using the algorithm in Fig. 5.

6. Task Driven MSBDL (TD-MSBDL)

In the following, we describe a task-driven extension of the MSBDL algorithm. For purposes of exposition, we assume the one-to-one prior in (12), but the approach applies equally to the priors discussed in Section 5. To incorporate task-driven learning, we modify the MSBDL graphical model to the one shown in Fig. 6. We set

$$p(q|x_j, W_j) = \mathbf{N}(q; W_j x_j, \beta_j^2 \mathbf{1}) \quad (57)$$

where β_j^2 is the class label noise variance for modality j . The class label noise variance is modality dependent, affording the model an extra level of flexibility compared to

11. This update rule assumes $J = 2$.

12. A balanced tree is one which has the same number of leaves for each subtree, or $|\mathcal{T}^k| = c$.

Require: $D, U, \{\mathcal{T}^k\}_{k=1}^K, M_p, S, \epsilon$

- 1: Let $z[m] = \|(S^T U)[m, :]\|_2^2 \forall m$
- 2: Let

$$v[k] = \arg \max_{m_1, m_2 \in \mathcal{T}^k \text{ s.t. } m_1 \neq m_2} \frac{|(d^{m_1})^T d^{m_2}|}{\|d^{m_1}\|_2 \|d^{m_2}\|_2} \quad (55)$$

- 3: **while** $\exists k$ s.t. $v[k] > \epsilon$ and $|\mathcal{T}^k| > 1$ and $M_p > 0$ **do**
- 4: $k = \arg \max_k v[k]$
- 5: Find $m = \arg \min_{m \in \mathcal{T}^k} z[m]$
- 6: Remove column m from D and \mathcal{T}^k
- 7: $M_p \leftarrow M_p - 1$
- 8: **end while**
- 9: **while** $M_p > 0$ **do**
- 10: Find

$$m = \arg \min_{m \in \mathcal{T}^k \text{ s.t. } |\mathcal{T}^k| > 1} z[m] \quad (56)$$

- 11: Remove column m from D and \mathcal{T}^k
- 12: $M_p \leftarrow M_p - 1$
- 13: **end while**
- 14: **return** D

Figure 5: Pruning algorithm for the learning strategy described in Section 5.3. The parameter M_p denotes the number of columns which must be pruned, S is given by the identity matrix for the atom-to-subspace model and by S_2 in (44) for the hierarchical sparsity model, and U denotes the matrix of first order sufficient statistics.

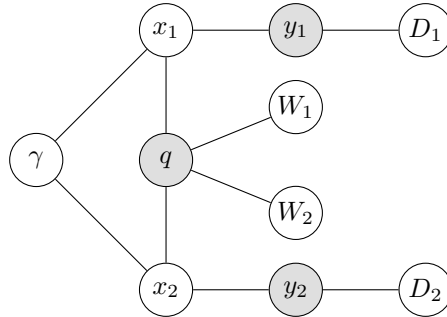


Figure 6: Graphical model for two modality TD-MSBDL.

(Bahrampour et al., 2016; Jiang et al., 2013; Mairal et al., 2012). The choice of the Gaussian distribution for the conditional density of \mathbf{q} , as opposed to a multinomial or softmax, stems from the fact that the posterior $p(x_j|y_j, q, D_j, W_j)$ needed to perform EM remains computable in closed form. In fact, it can be shown that

$$p(x_j^i|y_j^i, q, D_j, W_j) = \mathbf{N}\left(x_j^i; \Sigma_{x,j}^{TD,i}, \mu_j^{TD,i}\right) \quad (58)$$

where

$$\Sigma_{x,j}^{TD,i} = \left(\frac{D_j^T D_j}{\sigma_j^2} + \frac{W_j^T W_j}{\beta_j^2} + (\Gamma^i)^{-1} \right)^{-1} \quad (59)$$

$$\mu_j^{TD,i} = \Sigma_{x,j}^{TD,i} \left(\frac{D_j^T y_j^i}{\sigma_j^2} + \frac{W_j^T q^i}{\beta_j^2} \right) \quad (60)$$

6.1 Inference Procedure

We employ EM to seek

$$\arg \max_{\theta^{TD}} \log p\left(\{Y_j\}_{j=1}^J, Q|\theta^{TD}\right) \quad (61)$$

where $\theta^{TD} = \{\theta, \{W_j\}_{j=1}^J\}$. It can be shown that

$$p(y_j, q|x_j, \theta^{TD}) = \mathbf{N}\left(\begin{bmatrix} y_j^T & q^T \end{bmatrix}^T; 0, \Sigma_{y,j}^{TD}\right) \quad (62)$$

where

$$\Sigma_{y,j}^{TD} = \begin{bmatrix} \sigma_j^2 \mathbf{I} + D_j \Gamma D_j^T & 0 \\ 0 & \beta_j \mathbf{I} + W_j \Gamma W_j^T \end{bmatrix} \quad (63)$$

The update rules for $\{D_j\}_{j=1}^J$ and $\{\gamma^i\}_{i=1}^L$ ¹³ remain identical to (22) and (23), respectively, with the exception that the modified posterior statistics shown in (59)-(60) are used. The update of W_j is given by

$$W_j^{t+1} = Q (U_j^{TD})^T \left(U_j^{TD} (U_j^{TD})^T + \sum_{i=1}^L \Sigma_{x,j}^{TD,i} \right)^{-1} \quad (64)$$

$$U_j^{TD} = \begin{bmatrix} \mu_j^{TD,1} & \dots & \mu_j^{TD,L} \end{bmatrix}. \quad (65)$$

We also find it useful to add regularization in the form of $\nu \sum_{j=1}^J \|W_j\|_F^2$, leading to the update rule

$$W_j^{t+1} = \begin{bmatrix} Q (U_j^{TD})^T & 0 \end{bmatrix} \left(\begin{bmatrix} U_j^{TD} (U_j^{TD})^T + \sum_{i=1}^L \Sigma_{x,j}^{TD,i} & \\ & \sqrt{\nu} \mathbf{I} \end{bmatrix} \right)^{-1}. \quad (66)$$

TD-MSBDL has the same worst-case computational complexity as MSBDL with the benefit of supervised learning.

13. Assuming that the prior in (12) is used.

6.2 Complete Algorithm

Supervised learning algorithms are ultimately measured by their performance on test data. While a given algorithm may perform well on training data, it may generalize poorly to test data¹⁴. To maintain the generalization properties of the model, it is common to split the training data into a training set $\left\{ \{Y_j\}_{j=1}^J, Q \right\}$ and validation set $\left\{ \{Y_j^{val}\}_{j=1}^J, Q^{val} \right\}$, where the number of training points L does not necessarily have to equal the number of validation points L^{val} . The validation set is then used during the training process as an indicator of generalization, as summarized by the following rule of thumb: Continue optimizing θ^{TD} until performance on the validation set stops improving.

In the context of TD-MSBDL, the concept of generalization has a natural Bayesian definition: The parameter set $\left\{ \theta^{TD}, \{\beta_j\}_{j=1}^J \right\}$ which achieves optimal generalization is the solution of

$$\arg \max_{\theta^{TD} \in \mathcal{H}, \{\beta_j\}_{j=1}^J} \prod_{j=1}^J p\left(Q^{val} | \theta^{TD}, \beta_j\right) \quad (67)$$

where \mathcal{H} denotes the set of solutions to (61). Note that $p(Q^{val} | \theta^{TD}, \beta_j) = p(Q^{val} | W_j, \beta_j)$, which is intractable to compute since it requires integrating

$$p\left(q^{val,i} | W_j, \gamma^{val,i}, \beta\right) = \mathbf{N}\left(q^{val,i}; 0, \beta_j I + W_j \Gamma^{val,i} W_j^T\right), \quad \Gamma^{val,i} = \text{diag}(\gamma^{val,i}) \quad (68)$$

over $\gamma^{val,i}$. As such, we approximate $p(Q^{val} | W_j, \beta_j)$ by $p(Q^{val} | W_j, \gamma^{*,val,i}, \beta_j)$, where $\gamma^{*,val,i}$ is the output of the MSBDL algorithm with fixed D_j for input data $y_j^{val,i}$, leading to the tractable optimization problem

$$\arg \max_{\theta^{TD} \in \mathcal{H}, \{\beta_j\}_{j=1}^J} \prod_{j=1}^J p\left(Q^{val} | W_j, \{\gamma^{*,val,i}\}_{i=1}^{L^{val}}, \beta_j\right). \quad (69)$$

What remains is to define how to select $\{\beta_j\}_{j=1}^J$. As β_j decreases, TD-MSBDL fits the parameters θ^{TD} to the training data to a larger and larger degree, i.e. the optimizers of (61) achieve increasing objective function values. Since direct optimization of (69) over $\{\beta_j\}_{j=1}^J$ presents the same fundamental challenges as the optimization of $\{\sigma_j\}_{j=1}^J$ ¹⁵, we propose an annealing strategy which proposes progressively smaller values of β_j until the objective in (69) stops improving:

$$\beta_j^{t+1} = \begin{cases} \tilde{\beta}_j^{t+1} & \text{if } \log p\left(Q^{val} | W_j, \{\gamma^{*,val,i}\}_{i=1}^{L^{val}}, \tilde{\beta}_j^{t+1}\right) > \log p\left(Q^{val} | W_j, \{\gamma^{*,val,i}\}_{i=1}^{L^{val}}, \beta_j^t\right) \\ \beta_j^t & \text{else} \end{cases} \quad (70)$$

14. In the supervised learning community, lack of generalization to test data is commonly referred to as over-fitting the training data.

15. See Section 3.

Require: $\{Y_j, Y_j^{val}, \sigma_j^0, \beta_j^0, \sigma_j^\infty, \beta_j^\infty\}_{j=1}^J, Q, Q^{val}, \alpha_\sigma, \alpha_\beta, T^{val}$

- 1: **while** $\{\beta_j\}_{j=1}^J$ not converged **do**
- 2: **while** $\{D_j\}_{j=1}^J$ and $\{W_j\}_{j=1}^J$ not converged **do**
- 3: **for** $i \in [L]$ **do**
- 4: Update $\{\Sigma_{x,j}^{TD,i}\}_{j=1}^J$ using (59)
- 5: Update $\{\mu_j^{TD,i}\}_{j=1}^J$ using (20)
- 6: Update γ^i using (22)
- 7: **end for**
- 8: { Update D_j using (23) if σ_j not converged } $_{j=1}^J$
- 9: { Update W_j using (66) if β_j not converged } $_{j=1}^J$
- 10: **end while**
- 11: { Update σ_j using (30) if σ_j not converged } $_{j=1}^J$
- 12: **if** modulo(t, T^{val}) = 0 **then**
- 13: **for** $j \in [J]$ **do**
- 14: **if** β_j not converged **then**
- 15: $\{\gamma^{*,val,i}\}_{i=1}^{L^{val}} = MSBDL(Y_j^{val}, \sigma_j^0, \sigma_j, \sigma_j^\infty, \alpha_\sigma)$
- 16: Update β_j using (72)
- 17: **end if**
- 18: **end for**
- 19: **end if**
- 20: **end while**
- 21: **return** $\{D_j, W_j\}_{j=1}^J$

Figure 7: MSBDL algorithm for the prior in (12).

where $\beta_j^0 > \beta_j^\infty, \alpha_\beta < 1$,

$$\tilde{\beta}_j^{t+1} = \max(\beta_j^\infty, \alpha_\beta \beta_j^t). \quad (71)$$

Like in Section 3 , (70) can effectively be restated as

$$\beta^{t+1} = \begin{cases} \tilde{\beta}_j^{t+1} & \text{if } \frac{\partial \log p(Q^{val}|W_j^t, \beta_j^t)}{\partial \beta_j} < 0 \\ \beta_j^t & \text{else} \end{cases}. \quad (72)$$

Note that in this instance, (70) and (72) have the same computational complexity because both require running MSBDL. Since MSBDL is a computationally intensive operation, we only update the value of $\partial \log p(Q^{val}|W_j, \{\gamma^{*,val,i}\}_{i=1}^{L^{val}}, \tilde{\beta}_j^{t+1}) / \partial \beta_j$ every T^{val} iterations. The complete TD-MSBDL algorithm is summarized in Fig. 7.

6.3 Classifying Test Data

Given test data Y_j^{test} , we first run the MSBDL algorithm with D_j fixed and treat $\mu_j^{test,i}$ as an estimate of $x_j^{test,i}$. The data is then classified according to

$$\arg \max_{c \in [C]} \left(W_j \mu_j^{test,i} \right) [c] \quad (73)$$

where $[C] = \{1, \dots, C\}$ and e_c refers to the c 'th standard basis vector (Bahrapour et al., 2016).

7. Analysis

We begin by analyzing the convergence properties of MSBDL. Unless otherwise specified, the results hold for any choice of $p \left(\{\gamma\}_{j=1}^J \right)$. While MSBDL relies heavily on EM, it is not strictly an EM algorithm because of the σ annealing procedure. It will be shown that MSBDL still admits a convergence guarantee and an argument will be presented for why annealing σ tends to outperform a full EM treatment of the parameters¹⁶. Although we focus specifically on MSBDL, the results apply to TD-MSBDL.

First, consider the inner loop of the MSBDL algorithm in Fig. 2, where σ is held fixed while θ is updated. Proofs for all results are shown in the Appendix.

Theorem 1 *Without loss of generality, let $J = 1$ ¹⁷. Let σ be fixed and consider generating a sequence $\{\theta^t\}_{t=1}^\infty$ using the inner loop of the algorithm in Fig. 2. Let D^t be full rank for all t . Then, all of the limit points of $\{\theta^t\}_{t=1}^\infty$ are stationary points of $\log p(Y|\theta, \sigma)$ with respect to θ . Moreover, $\{\log p(Y|\theta^t, \sigma)\}_{t=1}^\infty$ converges monotonically to $\log p(Y|\theta^*, \sigma)$, where θ^* is a stationary point.*

Switching to the outer loop of Fig. 2, a much stronger property can be proven with respect to the convergence of σ .

Theorem 2 *Without loss of generality, let $J = 1$. Let θ be fixed,*

$$\sigma^0 \geq \arg \max_{\sigma} \log p(Y|\theta, \sigma), \quad (74)$$

α_σ be arbitrarily close to 1, and consider updating σ using the update rule in Fig. 2. Then, the following is guaranteed to be true:

- *If $\sigma^t \neq \sigma^{t-1}$, then $\log p(Y|\theta, \sigma^t) > \log p(Y|\theta, \sigma^{t-1})$*
- *If $\sigma^t = \sigma^{t-1}$, then $\sigma^t = \arg \max_{\sigma} \log p(Y|\theta, \sigma)$*

Theorem 3 *Without loss of generality, let $J = 1$. Let a non-informative prior be assumed for γ , $\|d^m\|_2 > 0 \forall m$, and $\exists i$ such that $\gamma^i[m] > 0$ for any choice of m . Then, $-\log p(Y|\theta, \sigma)$ is a coercive function of $\{\theta, \sigma\}$.*

16. We observe, experimentally, that the annealing procedure in (29) is superior to an EM treatment of σ .

17. When $J = 1$, we omit modality subscripts for brevity.

Corollary 1 *Let the conditions of Theorem 3 be satisfied. Then, the sequence of iterates $\{\theta^t, \sigma^t\}_{t=1}^\infty$ produced by the MSBDL algorithm in Fig. 2 admits at least one limit point.*

Theorem 4 *Without loss of generality, let $J = 1$. Let the conditions of Theorems 1, 2, and 3 be satisfied. Consider computing $\{\theta^t, \sigma^t\}_{t=1}^\infty$ using the algorithm in Fig. 2. Then, the sequence $\{\theta^t, \sigma^t\}_{t=1}^\infty$ converges to the set of stationary points of $\log p(Y|\theta, \sigma)$.*

Convergence results like Theorem 4 cannot be established for K-SVD and $J\ell_0$ DL because they rely on greedy search techniques. In addition, no convergence results are presented in (Bahrampour et al., 2016) for $J\ell_1$ DL.

Although Theorems 2-4 establish that MSBDL has favorable convergence properties, the question still remains as to why we choose to anneal σ instead of estimating it within EM. At a high level, it can be argued that setting σ to a (relatively) large value initially and then gradually decreasing it prevents MSBDL from getting stuck in poor stationary points at the beginning of the learning process. To motivate this intuition, consider the log likelihood function in (13). The curvature of the log-likelihood depends directly on σ . Setting a high σ corresponds to choosing a relatively flat log likelihood surface, which, from an intuitive point of view, has less stationary points. It is difficult to prove, in general, that $\log p(Y|\theta, \sigma_1)$ has less stationary points than $\log p(Y|\theta, \sigma_2)$ for $\sigma_1 > \sigma_2$. Nevertheless, a constrained case can be considered in order to give further weight to the annealing strategy.

Theorem 5 *Without loss of generality, let $J = 1$. Let σ_1, σ_2 be fixed, where $\sigma_1 > \sigma_2$. Let $\Psi = \{D : D = [\check{D} \ 1]\}$. Let $\Omega_\sigma = \{\Sigma_y : \Sigma_y = \sigma^2 I + D\Gamma D^T, D \in \Psi\}$. Then, $|\Omega_{\sigma_1}| \leq |\Omega_{\sigma_2}|$.*

Theorem 5 suggests that as σ gets smaller, the space over which the log-likelihood in (13) is optimized grows. As the optimization space grows, we conjecture that the number of stationary points grows as well. As a result, it may be advantageous to slowly anneal σ in order to allow MSBDL to learn D without getting stuck in a poor stationary point.

We now turn to the analysis of the proposed stochastic MSBDL approaches. Specifically, it is important to ask whether a convergence result similar to Theorem 1 can be given in the stochastic EM regime.

Theorem 6 *Without loss of generality, let $J = 1$. Let the prior on γ be separable and non-informative. Let σ be fixed and U^t be full rank for all t . Consider generating $\{\theta^t\}_{t=1}^\infty$ using the inner loop of the algorithm in Fig. 2, only updating the sufficient statistics for a batch of points ϕ at each iteration (i.e. incremental EM). Then, the limit points of $\{\theta^t\}_{t=1}^\infty$ are stationary points of $\log p(Y|\theta, \sigma)$ with respect to θ .*

7.1 Guarantees for multimodal dictionary recovery

Finally, we consider what guarantees can be given for dictionary recovery in the noiseless setting, i.e.

$$Y_j = D_j X_j \quad \forall j. \tag{75}$$

We assume $M_j = M \quad \forall j$ and that $\{x_j^i\}_{j=1}^J$ share a common sparsity profile for all i . We do not claim that the following result applies to more general cases when $M_j \neq M \quad \forall j$ or

different priors. The question we seek to answer is: Under what conditions is the factorization $Y_j = D_j X_j$ unique? Due to the nature of dictionary learning, uniqueness can only be considered up to permutation and scale. Two dictionaries D^1 and D^2 are considered equivalent if $D^1 = D^2 H$, where H is a permutation and scaling matrix. Guarantees of uniqueness in the unimodal setting were first studied in (Aharon et al., 2006b). The results relied on several assumptions about the data generation process.

Assumption 1 *Let $s = \|x_j^i\|_0 \forall i, j$, and let $s < \frac{\text{spark}(D_j)}{2}$, where $\text{spark}(D_j)$ denotes the minimum number of columns of D_j which are linearly dependent (Donoho and Elad, 2003). Each x_j^i has exactly s non-zeros.*

Assumption 2 *Y_j contains at least $s+1$ different points generated from every combination of s atoms of D_j .*

Assumption 3 *The rank of every group of $s+1$ points generated by the same s atoms of D_j is exactly s . The rank of every group of $s+1$ points generated by different atoms of D_j is exactly $s+1$.*

Lemma 7 (Theorem 3, (Aharon et al., 2006b)) *Let Assumptions 1-3 be true. Then, Y_j admits a unique factorization $D_j X_j$. The minimum number of samples required to guarantee uniqueness is given by $(s+1) \binom{M}{s}$.*

Treating the multimodal dictionary learning problem as J independent unimodal dictionary learning problems, following result follows from Lemma 7.

Corollary 2 *Let Assumptions 1-3 be true for all j . Then, Y_j admits a unique factorization $D_j X_j$ for all j . The minimum number of samples required to guarantee uniqueness is given by $J(s+1) \binom{M}{s}$.*

As the experiments in Section 8 will show, there are benefits to jointly learning multimodal dictionaries. It is therefore interesting to inquire whether or not there are *provable* benefits to the multimodal dictionary learning problem, at least from the perspective of the uniqueness of factorizations. To formalize this intuition, consider the scenario where some data points i do not have data available for all modalities. Let the Boolean matrix $P \in \mathbb{B}^{J \times L}$ be defined such that $P[j, i]$ is 1 if data for modality j is available for instance i and 0 else. The conditions on the amount of data needed to guarantee unique recovery of $\{D_j\}_{j=1}^J$ by Corollary 2 can be restated as $L = (s+1) \binom{M}{s}$ and $P[j, i] = 1 \forall j, i$. The natural question to ask next is: Can uniqueness of factorization be guaranteed if $P[j, i] = 0$ for some (j, i) ?

Theorem 8 *Let $\{x_j^i\}_{j=1}^J$ share a common sparsity profile for all i . Let Assumptions 1-2 be true for all j . Let Assumption 3 be true for a single modality, j^* . Let $G_j^k = \{i : P[j, i] = 1 \text{ and } y_j^i \in \text{span}(D_j[:, \Upsilon^k])\}$ where Υ^k is the k 'th subset of size s of $[M]$. Let $|G_j^k \cap G_{j^*}^k| \geq s$ for all $j \neq j^*$ and k . Then, the factorization $Y_j = D_j X_j$ is unique for all j . The minimum total number of data points required to guarantee uniqueness is given by $J(s + \frac{1}{J}) \binom{M}{s}$.*

Theorem 8 establishes that the number of samples required to guarantee a unique solution to the multimodal dictionary learning problem is *strictly less* than in Corollary 2 for $J > 1$.

8. Results

8.1 Synthetic Data Dictionary Learning

To validate how well MSBDL is able to learn unimodal and multimodal dictionaries, we conducted a series of experiments on synthetic data. We adopt the experimental setup from (Yang et al., 2016) and begin by generating the elements of the ground-truth dictionaries $D_j \in \mathbb{R}^{20 \times 50}$ by sampling from a $\mathcal{N}(0, 1)$ distribution and scaling the resulting matrices to have unit ℓ_2 column norm. We then generate x_j^i by randomly selecting $s = 5$ indices and generating the non-zero entries by drawing samples from a $\mathcal{N}(0, 1)$ distribution. The supports of $\{x_j^i\}_{j=1}^J$ are constrained to be the same, while the coefficients are not. Finally, the elements of v_j^i are generated by drawing samples from a $\mathcal{N}(0, 1)$ distribution and scaling the resulting vector in order to achieve a specified Signal-to-Noise Ratio (SNR). We use $L = 1000$ and simulate both bimodal ($J = 2$) and trimodal ($J = 3$) datasets. The bimodal dataset consists of 30dB ($j = 1$) and 10dB ($j = 2$) SNR modalities. The trimodal dataset consists of 30 dB ($j = 1$), 20 dB ($j = 2$), and 10 dB ($j = 3$) SNR modalities. We use the empirical probability of recovering $\{D_j\}_{j=1}^J$ as the measure of success, which is given by

$$\frac{1}{M_j} \sum_{m=1}^{M_j} \mathbb{1} \left[\iota \left(d_j^m, \hat{D}_j \right) > 0.99 \right] \quad (76)$$

where \hat{D}_j denotes the output of the dictionary learning algorithm,

$$\iota \left(d_j^m, \hat{D}_j \right) = \max_{1 \leq m' \leq M_j} \frac{\left| \left(d_j^m \right)^T \hat{d}_j^{m'} \right|}{\|d_j^m\|_2 \| \hat{d}_j^{m'} \|_2}, \quad (77)$$

and $\mathbb{1}[\cdot]$ denotes the indicator function. The experiment is performed 50 times and averaged results are reported.

We compare MSBDL with ℓ_1 DL, K-SVD, $J\ell_0$ DL, and $J\ell_1$ DL. Code for ℓ_1 DL was made available by the authors at <http://spams-devel.gforge.inria.fr/downloads.html>. Code for K-SVD was made available by the authors at <http://www.cs.technion.ac.il/~ronrubin/software.html>. While code for $J\ell_1$ DL was publicly available, it could not be run on any of our Windows or Linux machines, so we used our own implementation. Code for $J\ell_0$ DL was not publicly available, so we used our own implementation based on a block-coordinate descent optimization approach where the sparse coding step was computed using DC-SOMP and the dictionary update step was done using the same procedure as in K-SVD. For all algorithms, the batch size was set to L^{18} .

For the bimodal setting, the parameters σ_1^0 and σ_2^0 were set to 1 and 10, respectively. For the trimodal setting, the parameters σ_1^0 , σ_2^0 , and σ_3^0 were set to 1, 1.5, and 2, respectively. It was experimentally determined that MSBDL is relatively insensitive to the choice of σ_j^0 as long as $\sigma_1^0 < \sigma_2^0 < \sigma_3^0$, thus obviating the need to cross-validate these parameters. The regularization parameters λ in (2) and $\{\lambda_j\}_{j=2}^J$ in (5) were selected by a grid search over

18. When $L_0 = L$, MSBDL is equivalent to MSBDL-1.

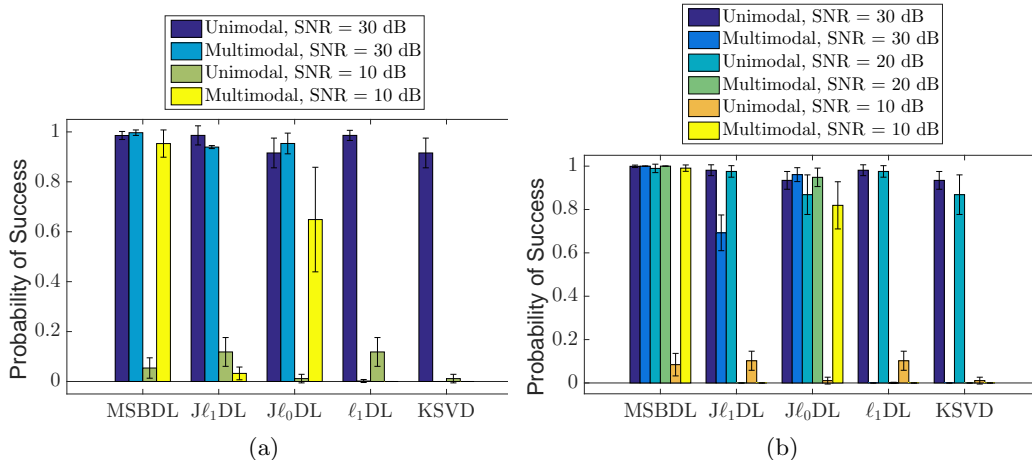


Figure 8: (8a) Bimodal synthetic data results with one standard deviation error bars. (8b) Trimodal synthetic data results with one standard deviation error bars.

$\{1e-3, 1e-2, 1e-1, 1\}$ and both K-SVD and $J\ell_0$ DL were given the true s . The parameter λ_1 was set to 1 for $J\ell_0$ DL across all experiments because the objective function in (5) depends only on the relative weighting of modalities. For multimodal dictionary learning, K-SVD was given data in the format \tilde{Y} , like in (2). All algorithms were run until convergence.

The bimodal and trimodal dictionary recovery results are shown in Fig.’s 8a and 8b, respectively. For unimodal data, all of the algorithms recover the true dictionary almost perfectly when the SNR = 30 dB, with the exception of $J\ell_0$ DL and K-SVD. All of the tested algorithms perform relatively well for data with 20 dB SNR and poorly on data with 10 dB SNR, although MSBDL outperforms the other tested method in these scenarios. In the multimodal scenario, the proposed method clearly distinguishes itself from the other methods tested. For trimodal data, not only does MSBDL achieve 100% accuracy on the 30 dB data dictionary, but it achieves accuracies of 100% and 99.2% on the 20 dB and 10 dB data dictionaries, respectively. MSBDL outperforms the next best method by 17.2% on the 10 dB data recovery task¹⁹ than the next best method. $J\ell_0$ DL was able to capture some of the multimodal information in learning the 10 dB data dictionary, but the 10 dB data dictionary accuracy only reaches 81.9%. $J\ell_1$ DL performs even worse in recovering the 10 dB data dictionary, achieving 0% accuracy. Similar trends can be seen in the bimodal results.

Next, we evaluate the performance of the MSBDL algorithms in Table 3a. We repeat the bimodal experiment and compare the proposed methods with $J\ell_1$ DL, which is the only competing multimodal dictionary learning algorithm that has a stochastic version. The dictionary recovery results are shown in Fig. 9. The results show that $J\ell_1$ DL is not able to recover any part of either the 30 dB nor 10 dB dataset dictionaries. In terms of the asymptotic performance as the batch size approaches L , MSBDL-1 exhibits negligible bias on both datasets, whereas the other MSBDL flavors incur a small bias, especially on the 10

19. Throughout this work, we report the improvement to the probability of success or the classification rate in absolute terms.

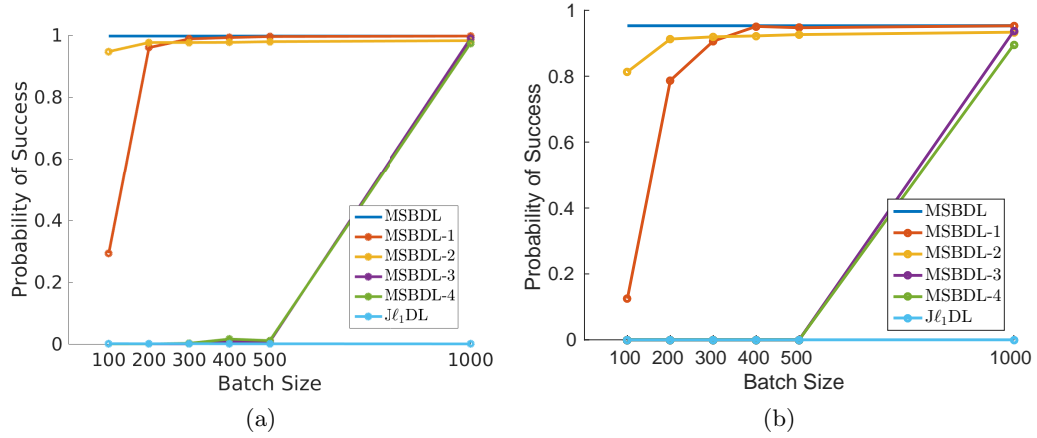


Figure 9: Bimodal synthetic data results using stochastic learning for 30 dB (Fig. 9a) and 10 dB (Fig. 9b) datasets.

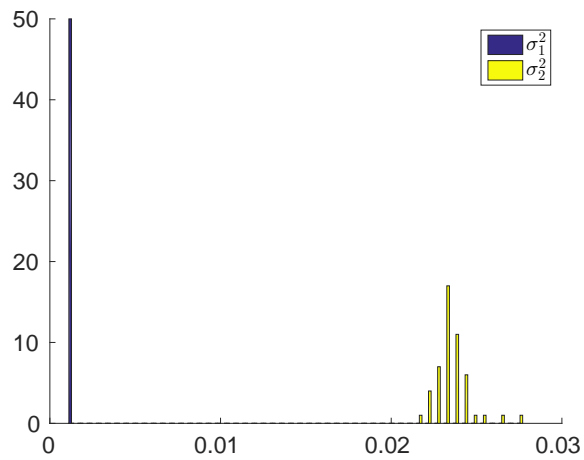


Figure 10: Histogram of σ_j^2 at convergence for a bimodal dataset consisting of 30 dB and 10 dB modalities.

dB dataset. On the other hand, it is interesting that MSBDL-2 dramatically outperforms MSBDL-1 for batch sizes less than 300, which is unexpected since MSBDL-2 performs approximate sufficient statistic computations. The poor performance of MSBDL-3 and MSBDL-4 suggests that these algorithms should be considered only in extremely memory constrained scenarios.

Finally, we report on the performance of the proposed annealing strategy for σ_j . For the bidomal dataset where the SNR of modality 1 is 30 dB and the SNR of modality 2 is 10 dB, one expects to see that σ_1 converges to a smaller value than σ_2 . Fig. 10 shows a histogram of the values to which $\{\sigma_j\}_{j=1}^J$ converge to²⁰. The results align with expectations and lend experimental validation for the annealing strategy. We observe the same trend for MSBDL-1 with $L_0 < L$.

8.2 Synthetic Data Dictionary Learning Under Atom-to-Subspace Model

To validate the performance of MSBDL using the atom-to-subspace model, we run a number of synthetic data experiments. In all cases, we use $J = 2$ and $L = 1000$. We use MSBDL-1 with $L_0 = 500$ to highlight that the algorithm works in incremental EM mode. We simulate 4 scenarios, summarized in Table 1. For each scenario, we first generate the elements of the ground-truth dictionary $\{D_j\}_{j=1}^J$ by sampling from a $\mathcal{N}(0, 1)$ distribution and normalizing the resulting dictionaries to have unit ℓ_2 column norm. We then set

$$\mathcal{T}^k = \begin{cases} \{k, k + M_1\} & \text{if } k + M_1 \leq M_2 \\ k & \text{else.} \end{cases} \quad (78)$$

This choice of $\{\mathcal{T}^k\}_{k=1}^K$ represents the most uniform assignment of columns of D_2 to columns of D_1 . We then generate x_1^i by randomly selecting $s = 5$ indices and generating the non-zero entries by drawing samples from a $\mathcal{N}(0, 1)$ distribution. We use $\{\mathcal{T}^k\}_{k=1}^K$ to find the support of x_2^i and generate the non-zero entries by drawing from a $\mathcal{N}(0, 1)$ distribution. Finally, the elements of v_j^i are generated by drawing from a $\mathcal{N}(0, 1)$ distribution and scaling the resulting vector to achieve the specified SNR. In order to assess the performance of the learning algorithm, we must first define the concept of the distance between multi-dimensional subspaces. In this work, we follow (Gunawan et al., 2005) and compute the distance between $D_2[:, \mathcal{T}^k]$ and \hat{D}_2 using

$$\iota(D_2[:, \mathcal{T}^k], \hat{D}_2) = \max_{1 \leq k' \leq K} \sqrt{|V_1^T V_2 V_2^T V_1|}, \quad (79)$$

where we use $D_2[:, \mathcal{T}^k]$ to denote the columns of D_2 indexed by \mathcal{T}^k , and V_1 and V_2 denote orthonormal bases for $D_2[:, \mathcal{T}^k]$ and $\hat{D}_2[:, \mathcal{T}^{k'}]$, respectively. We then define the distance between D_2 and \hat{D}_2 using the two quantities

$$\vartheta_{atom}(D_2, \hat{D}_2) = \frac{1}{|\{k : |\mathcal{T}^k| = 1\}|} \sum_{k \in \{k : |\mathcal{T}^k| = 1\}} \mathbb{1} \left[\iota(D_2[:, \mathcal{T}^k], \hat{D}_2) > 0.99 \right] \quad (80)$$

$$\vartheta_{subspace}(D_2, \hat{D}_2) = \frac{1}{|\{k : |\mathcal{T}^k| > 1\}|} \sum_{k \in \{k : |\mathcal{T}^k| > 1\}} \mathbb{1} \left[\iota(D_2[:, \mathcal{T}^k], \hat{D}_2) > 0.99 \right]. \quad (81)$$

20. We set $\sigma_j^\infty = 1e - 3 \forall j$ and $L = 1000$.

	d_1, M_1	d_2, M_2	SNR_1	SNR_2	$\vartheta_{atom}(D_1, \hat{D}_1)$	$\vartheta_{atom}(D_2, \hat{D}_2)$	$\vartheta_{subspace}(D_2, \hat{D}_2)$
A	20, 50	40, 100	30	30	99.8	—	92
B	20, 50	30, 60	30	30	99.5	100	97
C	20, 50	30, 60	30	10	99.9	68.05	3.6
D	20, 50	30, 60	10	30	73.64	97.7	75.4

Table 1: Recovery results on synthetic data using the atom-to-subspace model.

We use MSBDL-1 to learn $\{\hat{D}_j\}_{j=1}^J$, with accuracy results reported in Table 1 and visualized in Fig. 11 for a higher resolution perspective into the performance of the proposed approach. Note that Table 1 reports the accuracy of MSBDL-1 in recovering both the atoms and subspaces of D_2 . Test case A simulates the scenario where both modalities have a high SNR and $M_2 = 2M_1$. In other words, test case A tests if MSBDL-1 is able to learn in the atom-to-subspace model, without the complications that arise from added noise. The results show that MSBDL-1 effectively learns both the atoms of D_1 and the subspaces comprising D_2 . Test case B simulates the scenario where $|\mathcal{T}^k| = 1$ for some k but not for others. In effect, test case B tests the pruning strategy described in Section 5.3 and summarized in Fig. 5. The results show that the pruning strategy is effective and allows MSBDL-1 to learn both the atoms of D_1 and the atoms and subspaces comprising D_2 . Test case C is identical to test case B, but with noise added to modality 2. The results show that MSBDL-1 still effectively recovers D_1 , but there is a drop in performance with respect to recovering the atoms of D_2 and a significant drop in recovering the subspaces of D_2 . Nevertheless, inspecting Fig. 11g-11h, we see that the distribution of $\iota(\cdot, \cdot)$ between the atoms and subspaces, respectively, of the true and estimated dictionaries is concentrated near 1 for test case C. Finally, test case D considers the scenario where the modality comprising the roots of the tree is noisy. The results show that MSBDL-1 performs robustly in this scenario.

To provide experimental evidence for the fact that the atom-to-subspace model is agnostic to the atoms of D_2 , as discussed in Section 5.1, we show the ability of MSBDL-1 to recover the atoms of D_2 for test case A in Fig. 12. The results show that MSBDL-1 is not able to recover the atoms of D_2 even in the absence of noise.

8.3 Synthetic Data Dictionary Learning Under Hierarchical Model

In this section, we present experimental results for dictionary learning under the hierarchical model. In all cases, we use $J = 2$, $L = 1000$, and MSBDL-1 with $L_0 = 500$. We simulate 4 scenarios, summarized in Table 2. The ground truth dictionaries are generated in the same way as Section 8.2, including the choice of \mathcal{T}^k shown in (78). To evaluate the performance of the proposed approach, we measure how well it is able to recover the atoms of D_1 and D_2 , where we distinguish between the atoms of D_2 corresponding to $|\mathcal{T}^k| = 1$ and $|\mathcal{T}^k| > 1$

	d_1, M_1	d_2, M_2	SNR_1	SNR_2	$\vartheta_{atom}(D_1, \hat{D}_1)$	$\vartheta_{atom}^1(D_2, \hat{D}_2)$	$\vartheta_{atom}^1(D_2, \hat{D}_2)$
A	20, 50	40, 100	30	30	99.3	—	96.6
B	20, 50	30, 60	30	30	100	94.7	82.7
C	20, 50	30, 60	30	10	100	22.1	3.3
D	20, 50	30, 60	10	30	5.2	93.1	61.1

Table 2: Recovery results on synthetic data using the hierarchical model.

using

$$\vartheta_{atom}^1(D_2, \hat{D}_2) = \frac{1}{|\{k : |\mathcal{T}^k| = 1\}|} \sum_{k \in \{k : |\mathcal{T}^k| = 1\}} \mathbb{1} \left[\iota(D_2[:, \mathcal{T}^k], \hat{D}_2) > 0.99 \right] \quad (82)$$

$$\vartheta_{atom}^2(D_2, \hat{D}_2) = \frac{1}{\sum_{k: |\mathcal{T}^k| > 1} |\mathcal{T}^k|} \sum_{k \in \{k : |\mathcal{T}^k| > 1\}} \sum_{m \in \mathcal{T}^k} \mathbb{1} \left[\iota(D_2[:, m], \hat{D}_2) > 0.99 \right]. \quad (83)$$

The recovery results are reported in Table 2 and visualized in Fig. 13. Test case A demonstrates that MSBDL-1 is able to learn the atoms of D_1 and D_2 in the low noise scenario for $M_2 = 2M_1$. Test case B shows that MSBDL-1 is able to learn the atoms of D_1 and D_2 for $M_1 < M_2 < 2M_1$, i.e. highlighting that the pruning strategy in Fig. 5 is effective for the hierarchical sparsity model. Test case C adds a considerable amount of noise to the modality occupying the leaves of the tree. Although the recovery results in Table 2 suggest that MSBDL-1 does not perform well in recovering D_2 in this scenario, the histograms in Fig.’s 13g-13h show that the distribution of $\iota(\cdot, \cdot)$ is concentrated near 1 for subtrees satisfying both $|\mathcal{T}^k| = 1$ and $|\mathcal{T}^k| > 1$. Finally, test case D shows the scenario where a large amount of noise is added to the modality occupying the roots of each subtree. The results in Fig.’s 13j-13k show that MSBDL-1 performs reasonably in the recovery of both D_1 and D_2 under these challenging conditions.

8.4 Photo Tweet Dataset Classification

We validate the performance of TD-MSBDL by running it on the Photo Tweet dataset (Borth et al., 2013). The Photo Tweet dataset consists of 603 tweets covering 21 topics. Each tweet contains text and an image with an associated binary label indicating whether the tweet represents a positive sentiment or not. The dataset consists of 5 partitions. We use these partitions to perform 5 rounds of leave-one-out cross-validation, where, during each round, we use one partition as the test set, one as the validation set, and the remaining partitions as the training set. For each round, we process the images by first extracting a bag of SURF features (Bay et al., 2006) from the training set using the MATLAB computer vision system toolbox. We then encode the training, validation, and test sets using the learned bag of features, generating a 500-dimensional representation for each image (Csurka et al., 2004). Finally, we compute the mean of each dimension across the training set, center the training, validation, and test sets using the computed means, and perform 10 component PCA to generate a 10-dimensional image representation. We process the text data by first building a 2688 dimensional bag of words from the training set using the scikit-learn Python library. We then encode the training, validation, and test sets us-

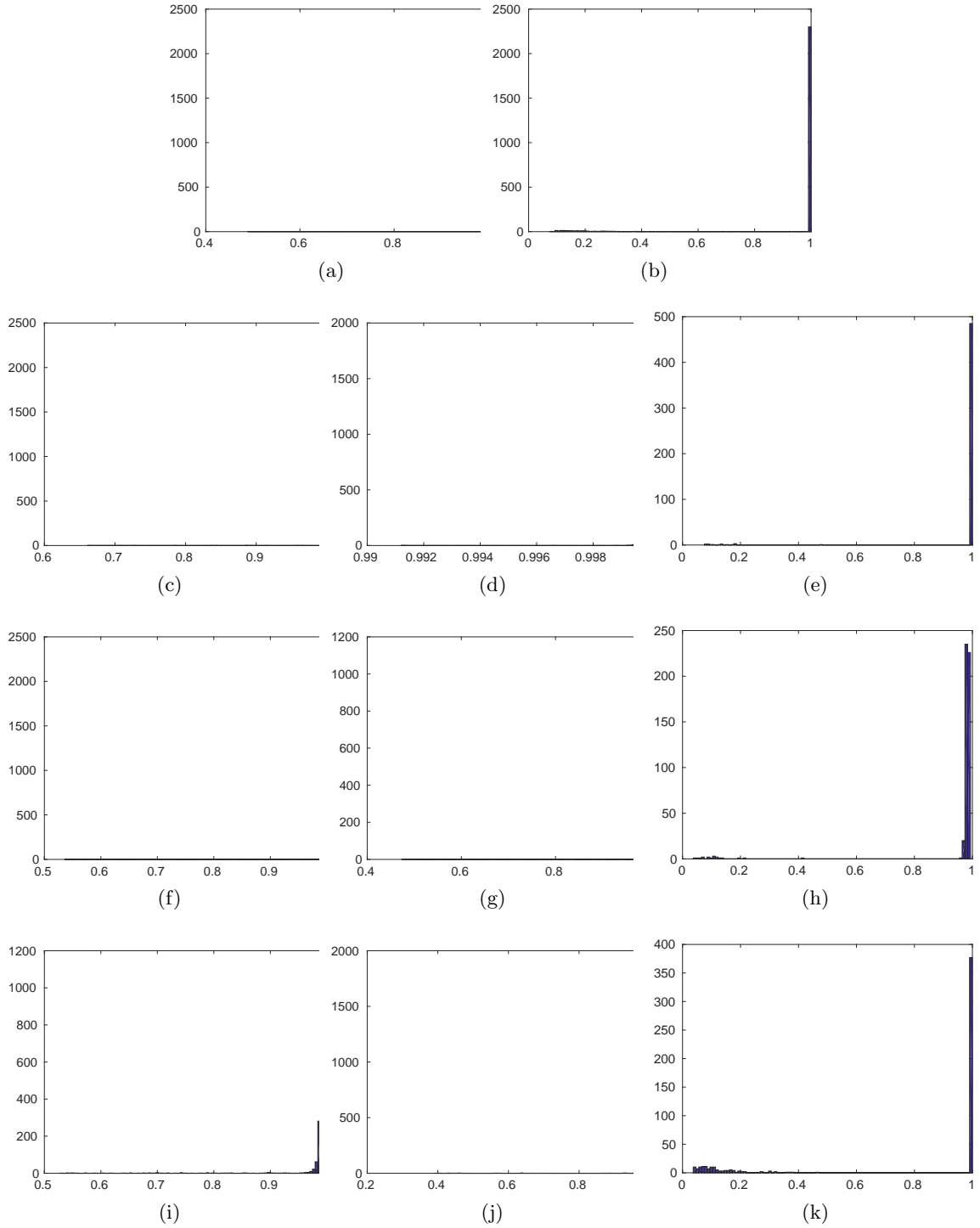


Figure 11: Histograms of dictionary recovery results for the atom-to-subspace model and test cases in Table 1. (Fig.'s 11a, 11c, 11f, 11i): distribution of $\iota(D_1[:, m], \hat{D}_1) \forall m$ for cases A-D, respectively. (Fig.'s 11d, 11g, 11j): distribution of $\iota(D_2[:, k], \hat{D}_2) \forall k : |\mathcal{T}^k| = 1$ for cases B-D, respectively. (Fig.'s 11b, 11e, 11h, 11k): distribution of $\iota(D_2[:, k], \hat{D}_2) \forall k : |\mathcal{T}^k| > 1$ for cases A-D, respectively.

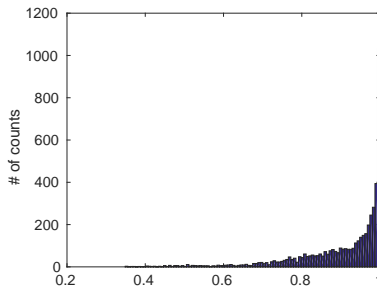


Figure 12: Histogram of $\iota(D_2[:, m], \hat{D}_2) \forall m$ for test case A.

ing the learned bag of words, normalizing the resulting representations by the number of words in the tweet. We then center the data and perform 10 component PCA to generate a 10-dimensional text representation.

We run TD-MSBDL using incremental EM and approximate posterior sufficient statistic computations, referring to the resulting algorithm as TD-MSBDL-3 in accordance with the taxonomy in Table 3a. Our convention is to refer to the text and image data as modalities 1 and 2 respectively. We use $M_j = 40 \forall j$, $L_0 = 200$, $\sigma_1^0 = 0.01$, $\sigma_2^0 = 0.2$, $\beta_j^0 = 100 \forall j$, $\sigma_j^\infty = 1e - 4 \forall j$, $\beta_j^\infty = 1e - 2 \forall j$, and $T^{val} = 500$.

We compare TD-MSBDL with several unimodal and multimodal approaches. We use TD- ℓ_1 DL and D-KSVD to learn classifiers for images and text using unimodal data. For TD- ℓ_1 DL we use the validation set to optimize for λ over the set $\{1e-3, 1e-2, 1e-1, 1\}$. We also compare with TD-J ℓ_1 DL trained on the multimodal data. We use the same validation approach as for TD- ℓ_1 DL. In all cases, we run training for a maximum of 15e3 iterations.

The classification results are shown in Table 3. Comparing TD-MSBDL with the unimodal methods (i.e. TD- ℓ_1 DL and D-KSVD), the results show that TD-MSBDL achieves higher performance for both feature types. Moreover, it is interesting that TD-J ℓ_1 DL performs worse than TD- ℓ_1 DL, suggesting that it is not capable of capturing the multimodal relationships which TD-MSBDL benefits from.

8.5 Classification with atom-to-subspace and hierarchical sparsity priors

Finally, we show the efficacy of the priors in Section 5 in classifying the Photo Tweet dataset. The goal is to show that, by allowing the number of atoms of the image and text dictionaries to be different, the atom-to-subspace and hierarchical sparsity priors lead to superior classification performance.

We begin by extracting features from the text and image data using the method described in Section 8.4, with the exception that we use 20 PCA components to represent images. We then set M_1 , the text data dictionary size, to 40 and M_2 , the image dictionary size, to 80, corresponding to an oversampling factor M_j/N_j of 4 for both modalities. We run the TD-MSBDL algorithm in Fig. 7 with the atom-to-subspace and hierarchical sparsity priors. For the atom-to-subspace prior, the only required modification to the TD-MSBDL

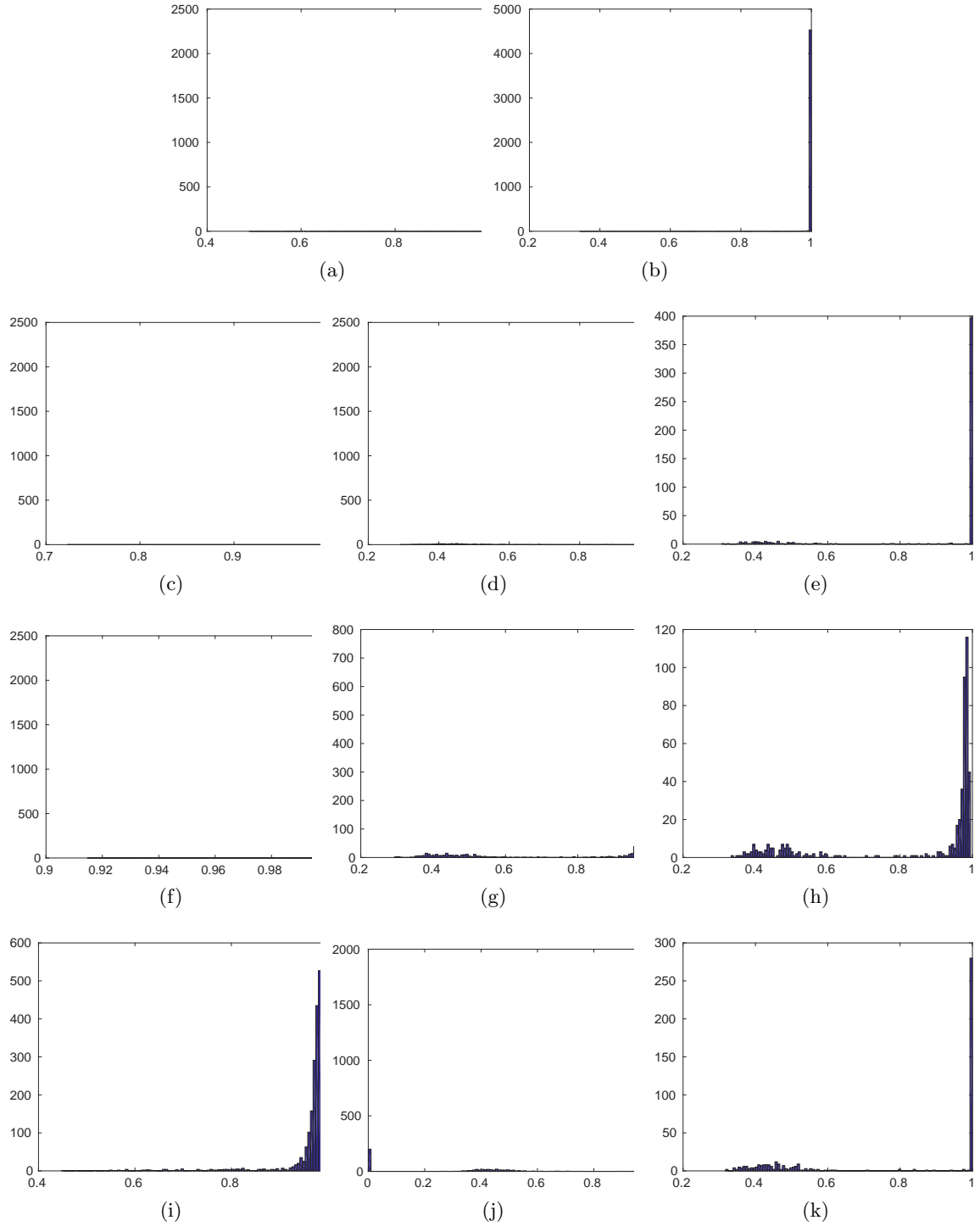


Figure 13: Histograms of dictionary recovery results for the atom-to-subspace model and test cases in Table 2. (Fig.'s 13a, 13c, 13f, 13i): distribution of $\iota(D_1[:, m], \hat{D}_1) \forall m$ for cases A-D, respectively. (Fig.'s 13d, 13g, 13j): distribution of $\iota(D_2[:, k], \hat{D}_2) \forall k : |\mathcal{T}^k| = 1$ for cases B-D, respectively. (Fig.'s 13b, 13e, 13h, 13k): distribution of $\iota(D_2[:, m], \hat{D}_2) \forall m \in T^k : |\mathcal{T}^k| > 1$ for cases A-D, respectively. 32

Feature Type	TD-MSBDL-3	TD- $J\ell_1$ DL	TD- ℓ_1 DL	D-KSVD
Images	65.6	59.2	61.1	63.9
Text	76	73.7	74.1	69.4

Table 3: Photo tweet dataset classification accuracy (%) using TD learning.

	TD-MSBDL-3	TD-MSBDL-1	TD-MSBDL-1
Prior	One-to-one (12)	Hierarchical (45)	Atom-to-subspace (37)
$d_1 \times M_1/d_2 \times M_2$	$10 \times 40/10 \times 40$	$10 \times 40/20 \times 80$	$10 \times 40/20 \times 80$
Images	65.6	69.2	69.5
Text	76	74.6	74.3

Table 4: Photo tweet dataset classification accuracy (%) using TD learning and priors from Section 5. Our convention is to designate text as modality 1 and images as modality 2.

algorithm in Fig. 7 is to change the update rule of γ^i to (22)²¹. For the hierarchical sparsity prior, the γ^i , D_j , and W_j update rules are modified to (53), (84), and

$$(W_j)^{t+1} = Q (U_j^{TD})^T S_j \left(S_j^T \left(U_j^{TD} (U_j^{TD})^T + \sum_{i=1}^L \Sigma_{\hat{x},j}^{TD,i} \right) S_j \right)^{-1}, \quad (84)$$

respectively. We set the algorithm hyperparameters to the same values as in Section 8.4, with the exception that $\beta_j^0 = 10 \forall j$ for the atom-to-subspace prior. Because there are significant dependencies among the elements in x_j a-priori, we use the MSBDL-1 flavor of MSBDL instead of MSBDL-3.

The classification results are presented in Table 4, where the TD-MSBDL-3 results with one-to-one prior from Section 8.4 are shown for reference. The results show a significant improvement in image classification. Although text classification deteriorates slightly, the text classification rate for both atom-to-subspace and hierarchical priors is still higher than any of the competing methods in Table 3.

9. Conclusion

We have detailed a sparse multimodal dictionary learning algorithm. Our approach incorporates the main features of existing methods, which establish a correspondence between the elements of the dictionaries for each modality, while addressing the major drawbacks of previous algorithms. Our method enjoys the theoretical guarantees and superior sparse recovery rates associated with the sparse Bayesian learning framework.

Appendix A. Proof of Theorem 1

The result stated in Theorem 1 follows directly from [Theorem 2, (Wu, 1983)] if it can be shown that $Q(\theta, \theta^t)$, defined in (18), is continuous in both θ and θ^t . First, consider the

21. We also found it necessary to introduce a post-processing step to the output of the TD-MSBDL algorithm with the atom-to-subspace prior. Specifically, the TD-MSBDL algorithm outputs the W_j^t which corresponds to the maximum measured classification accuracy on the validation set during training.

dependence of $Q(\theta, \theta^t)$ on $\gamma^i[m]$, which is given by

$$-\frac{\log \gamma^i[m]}{2} - \left(\frac{\Sigma_x^i[m, m] + (\mu^i[m])^2}{2\gamma^i[m]} \right) \quad (85)$$

where Σ_x^i and μ^i are given by (20) and (21), respectively, and depend on θ^t . It suffices to show that (85) is continuous on the open interval $(0, \infty]$. Since both $\log(\cdot)$ and $(\cdot)^{-1}$ are continuous functions on the interval $(0, \infty]$, it follows that (85) is continuous in $\gamma^i[m]$. The dependence of $Q(\theta, \theta^t)$ on D is given by

$$\sum_{i=1}^L (y^i)^T D \mu^i - \frac{\text{tr} \left((D^T D (\Sigma_x^i + \mu^i (\mu^i)^T)) \right)}{2} \quad (86)$$

which is continuous in D . Next, we turn to the task of showing that $Q(\theta, \theta^t)$ is continuous in θ^t , which reduces to showing that Σ_x^i is continuous in both D^t and γ^t . Let B be the matrix being inverted in (20):

$$B = \sigma^2 I + D^t \Gamma^{t,i} (D^t)^T. \quad (87)$$

The task then reduces to showing that $(B)^{-1}$ is continuous in D^t and $\gamma^{t,i}$. We first show that $(B)^{-1}$ exists. Using the assumption that D^t is full rank, B is full rank over $\gamma \in (0, \infty]^M$ since

$$\text{rank}(B) \geq \text{rank} \left(D^t \Gamma^{t,i} (D^t)^T \right) \quad (88)$$

$$= \text{rank} \left(D^t (\Gamma^{t,i})^{\frac{1}{2}} \left(D^t (\Gamma^{t,i})^{\frac{1}{2}} \right)^T \right) \quad (89)$$

$$= \text{rank} \left(D^t (\Gamma^{t,i})^{\frac{1}{2}} \right) \quad (90)$$

$$= N \quad (91)$$

where $(\Gamma^{t,i})^{\frac{1}{2}}$ is a diagonal matrix with the m 'th diagonal entry given by $\sqrt{\gamma^{t,i}[m]}$. Therefore, B is full rank and admits an inverse.

Since B is continuous in D^t and γ^t , what remains to be shown is that $(B)^{-1}$ is continuous in B . This follows from the fact that $(B)^{-1}$ can be expressed as

$$(B)^{-1} = \frac{1}{|B|} \text{adj}(B) \quad (92)$$

where $\text{adj}(B)$ is the adjugate of B . Since both the determinant and adjugate are continuous mappings (Gentle, 2007), it follows that $(B)^{-1}$ is continuous in B and, consequently, that $Q(\theta, \theta^t)$ is continuous in θ^t .

Appendix B. Proof of Theorem 2

We begin by proving the first guarantee of Theorem 2 that $\log p(Y|D, \gamma, \sigma^t) > \log p(Y|D, \gamma, \sigma^{t-1})$ if $\sigma^t \neq \sigma^{t-1}$. In fact, this result follows by construction since the update rule for σ in the MSBDL algorithm in Fig. 2 only updates σ if $\log p(Y|D, \gamma, \sigma^t) > \log p(Y|D, \gamma, \sigma^{t-1})$.

The second guarantee in Theorem 2 requires more careful consideration. Let σ^* be the local maximum of $\log p(Y|\theta, \sigma)$ closest to σ^0 . Let t^* satisfy

$$\sigma^{t^*-1} = \frac{\sigma^*}{\alpha_\sigma}. \quad (93)$$

A t^* satisfying (93) is guaranteed to exist because $\sigma^0 > \sigma^*$ and α_σ is allowed to be arbitrarily close to 1. Therefore, $\sigma^{t^*} = \sigma^*$ under the update rule in Fig. 2. In other words, the update rule in Fig. 2 is guaranteed to converge to a local maximum of $\log p(Y|\theta, \sigma)$ with respect to σ . What remains to be shown is that this local maximum is actually a global maximum of the log-likelihood. To prove this, we start by observing that the log-likelihood depends on σ through the covariance matrices $\{\Sigma_y^i\}_{i=1}^L$ shown in (16). If we parametrize $p(y^i; \Sigma_y^i)$ by the precision matrix $\Lambda^i = (\Sigma_y^i)^{-1}$, then it can be shown that $\log p(y^i; \Lambda^i)$ is a strictly concave function of Λ^i . Since the log-likelihood of Y is a sum of such functions, $\log p(Y|\{\Lambda^i\}_{i=1}^L)$ is itself a strictly concave function. Therefore, $\log p(Y|\{\Lambda^i\}_{i=1}^L)$ admits a single local maximum $\{\Lambda^{i,*}\}_{i=1}^L$, which is also its global maximum. Since the mapping from Λ^i to Σ_y^i is one-to-one, we conclude that $\log p(Y|\{\Sigma_y^i\}_{i=1}^L)$ also admits a single local maximum, which is also a global maximum. In other words, $\log p(Y|\{\Sigma_y^i\}_{i=1}^L)$ is a strictly quasiconcave function (Boyd and Vandenberghe, 2004). Consider maximizing the log-likelihood over the convex set $\Sigma_y^i \in \{\sigma^2 I + D\Gamma^i D^T : \sigma > 0\}$. Quasiconcave functions admit a single local maximum, which is also the global maximum, over convex sets (Boyd and Vandenberghe, 2004). We conclude that $\log p(Y|\{\Sigma_y^i\}_{i=1}^L)$ admits a single local maximum with respect to σ , which completes the proof.

Appendix C. Proof of Theorem 3

By definition, the log-likelihood function is coercive if

$$\lim_{\|\{\theta, \sigma\}\| \rightarrow \infty} -\log p(Y|\theta, \sigma) = \infty \quad (94)$$

where we define the norm of $\{\theta, \sigma\}$ to be

$$\|\{\theta, \sigma\}\| = \sqrt{\|\theta\|^2 + \sigma^2} \quad (95)$$

$$= \sqrt{\sum_{m=1}^M \|d^m\|_2^2 + \sum_{i=1}^L \|\gamma^i\|_2^2 + \sigma^2}. \quad (96)$$

The negative log-likelihood can be written as

$$-\log p(Y|\theta, \sigma) \doteq \sum_{i=1}^L (y^i)^T (\Sigma_y^i)^{-1} y + \log |\Sigma_y^i| \quad (97)$$

where \doteq refers to dropping terms which do not depend on θ or σ .

Next, we establish several results about Σ_y^i , which is defined in (16). Let $(\Gamma^i)^{0.5}$ be a diagonal matrix whose $[m, m]$ 'th entry is given by $(\gamma^i[m])^{0.5}$. Then, $D\Gamma^i D^T$ is the Gramian matrix of $(\Gamma^i)^{0.5} D^T$. Since Gramian matrices are positive semi-definite (PSD), $D\Gamma D^T$ must be PSD. Since $\sigma^2 I$ is PSD, Σ_y^i is PSD. Finally, since Σ_y^i is PSD, then $(\Sigma_y^i)^{-1}$ is also PSD. Therefore,

$$(y^i)^T (\Sigma_y^i)^{-1} y \geq 0 \quad (98)$$

in general.

Turning to the second term in (97), we can re-write it as

$$\log |\Sigma_y^i| = N\sigma^2 + \sum_{n=1}^N \lambda^i[n] \quad (99)$$

where $\lambda^i[n] \geq 0$ denotes the n 'th eigenvalue of $D\Gamma^i D^T$. Concentrating on the second term in (99), we have

$$\sum_{n=1}^N \lambda^i[n] = \text{trace}(D\Gamma^i D^T) \quad (100)$$

$$= \sum_{n=1, m=1}^{N, M} \gamma^i[m] (d^m[n])^2 \quad (101)$$

$$= \sum_{m=1}^M \gamma^i[m] \|d^m\|_2^2. \quad (102)$$

Combining (98) with (102), (97) can be re-written as

$$-\log p(Y|\theta, \sigma) \geq LN\sigma^2 + \sum_{i=1, m=1}^{L, M} \gamma^i[m] \|d^m\|_2^2. \quad (103)$$

In order for $\|\{\theta, \sigma\}\| \rightarrow \infty$, one or more of the terms under the square root in (95) must also approach infinity. Starting with σ , we have

$$\lim_{\sigma \rightarrow \infty} -\log p(Y|\theta, \sigma) = \infty \quad (104)$$

for any (valid) choice of θ . Turning to γ , we observe that in order for $\|\gamma^i\|_2^2 \rightarrow \infty$, there must exist at least one i^* and m^* such that $\gamma^{i^*}[m^*] \rightarrow \infty$. As a result,

$$\lim_{\gamma^{i^*}[m^*] \rightarrow \infty} -\log p(Y|\theta, \sigma) \geq \lim_{\gamma^{i^*}[m^*] \rightarrow \infty} \gamma^{i^*}[m^*] \|d^{m^*}\|_2^2 \quad (105)$$

$$=^a \infty \quad (106)$$

where step (a) follows from the assumption that $\|d^m\|_2^2 > 0 \forall m$. Finally, we examine the limit as $\|d^{m^*}\|_2^2 \rightarrow \infty$ for some m^* :

$$\lim_{\|d^{m^*}\|_2^2 \rightarrow \infty} -\log p(Y|\theta, \sigma) \geq \lim_{\|d^{m^*}\|_2^2 \rightarrow \infty} \left\| d^{m^*} \right\|_2^2 \sum_{i=1}^L \gamma^i[m^*] \quad (107)$$

$$=^a \infty \quad (108)$$

where step (a) follows from the assumption that at least one of $\{\gamma^i[m]\}_{i=1}^L$ is non-zero for all m .

Appendix D. Proof of Corollary 1

This proof follows closely to the first part of the proof of (Theorem 1, (Zhao and Tan, 2016)). Let

$$\mathcal{S}_0 = \{ \{\theta, \sigma\} : -\log p(Y|\theta, \sigma) \leq -\log p(Y|\theta^0, \sigma^0) \}, \quad (109)$$

where θ^0 and σ^0 denote the initial values of θ and σ , respectively. Theorem 3 established that $-\log p(Y|\theta, \sigma)$ is coercive. In addition, assume, for now, that $-\log p(Y|\theta, \sigma)$ is a continuous function of $\{\sigma, \theta\}$. Under these conditions, \mathcal{S}_0 is a compact set (Theorem 1.2, (Burke)). The sequence $\{-\log p(Y|\theta^t, \sigma^t)\}_{t=1}^\infty$ is non-increasing as a result of Theorems 1-2, such that $\{\theta^t, \sigma^t\}_{t=1}^\infty \in \mathcal{S}_0$. Since \mathcal{S}_0 is compact, $\{\theta^t, \sigma^t\}_{t=1}^\infty$ admits at least one limit point.

What remains is to show that $-\log p(Y|\theta, \sigma)$ is continuous. The continuity of the negative log-likelihood follows directly from the fact that both the determinant and matrix inverse functions are continuous²².

Appendix E. Proof of Theorem 4

This follows directly from [Theorem 2, (Wu, 1983)], whose conditions are satisfied as a consequence of Theorem 1 and Theorem 2.

Appendix F. Proof of Theorem 5

We will show that any point in Ω_{σ_1} must be in Ω_{σ_2} . Let the operator $\Theta_l : \mathbb{R}^{M \times M} \rightarrow \mathbb{R}^{M-N \times M-N}$ be defined such that $\Theta_l(\Gamma)$ extracts the top left $M-N \times M-N$ submatrix of Γ . Let the operator $\Theta_h : \mathbb{R}^{M \times M} \rightarrow \mathbb{R}^{N \times N}$ be defined such that $\Theta_h(\Gamma)$ extracts the bottom right $N \times N$ submatrix of Γ . Using these operators, we can express any element of Ω_σ as

$$\Sigma_y = (\sigma^2 \mathbf{1} + \Theta_h(\Gamma)) + \check{D} \Theta_l(\Gamma) \check{D}^T. \quad (110)$$

22. See [Theorem 5.19 (Schott, 2016)] and [Theorem 5.20 (Schott, 2016)] for continuity of the matrix determinant and inverse functions, respectively.

Let $\Sigma_{y,1}(D_1, \gamma_1) \in \Omega_{\sigma_1}$, where $\Sigma_y(\cdot, \cdot)$ denotes the dependence of Σ_y on D and γ . We can then show that $\Sigma_{y,1}(D_1, \gamma_1) = \Sigma_{y,2}(D_2, \gamma_2) \in \Omega_2$ for

$$\gamma_2[m] = \begin{cases} \gamma_1[m] & \text{if } m \leq M - N \\ \gamma_1[m] + \sigma_1^2 - \sigma_2^2 & \text{else} \end{cases}$$

and $\check{D}_2 = \check{D}_1$. Such a choice of $\Sigma_{y,2}(D_2, \gamma_2)$ is always possible because $\sigma_1 > \sigma_2$. The converse is not true for arbitrary choices of D_1 and γ_1 , leading to the set relation $|\Omega_{\sigma_1}| \leq |\Omega_{\sigma_2}|$.

Appendix G. Proof of Theorem 6

The guarantee given in Theorem 6 follows directly from [Proposition 6, (Gunawardana and Byrne, 2005)] if we can show that $Q(\theta, \theta^t)$ has a unique maximizer with respect to θ . Consider the optimization of $Q(\theta, \theta^t)$ with respect to D . This optimization problem can be rewritten as

$$\arg \max_D \sum_{i=1}^L - (y^i)^T D \mu^i + D \left(\Sigma_x^i + \mu^i (\mu^i)^T \right). \quad (111)$$

Since (111) is an unconstrained optimization problem, its maxima must occur at stationary points of the objective function. Taking the gradient of the objective function in (111) with respect to D and setting the result to zero, we get

$$D \underbrace{\left(UU^T + \sum_{i=1}^L \Sigma_x^i \right)}_B = YU^t \quad (112)$$

If B is invertible, all of the stationary points of the objective function in (111) have the form $YU(B)^{-1}$. Since Y, U are fixed and $(B)^{-1}$ is unique given U and $\{\Sigma_x^i\}_{i=1}^L$, we conclude that the objective function in (111) has exactly one, unique stationary point. In order to show that B is invertible, we observe that Σ_x^i is positive semi-definite for all i and U is full rank by assumption. Since the sum of a positive semi-definite and positive definite matrix is positive definite, it follows that B is invertible.

We now turn to the optimization of $Q(\theta, \theta^t)$ with respect to $\gamma^i[m]$ (since $Q(\theta, \theta^t)$ is separable in the elements of γ^i). This optimization problem can be rewritten as

$$\arg \max_{\gamma^i[m] \geq 0} - \frac{\log \gamma^i[m]}{2} - \left(\frac{\Sigma_x^i[m, m] + (\mu^i[m])^2}{2\gamma^i[m]} \right). \quad (113)$$

Note that we explicitly state the constraint on $\gamma^i[m]$. Since (113) is a constrained optimization problem, the global maxima can occur at stationary points of the objective function or at the constraint boundaries, i.e. $\gamma^i[m] = 0$. Stationary points of the objective function in (113) occur at

$$\gamma^i[m] = \Sigma_x^i[m, m] + (\mu^i[m])^2. \quad (114)$$

Consider, first, the case where $\Sigma_x^i[m, m] + (\mu^i[m])^2 = 0$. In this instance, the stationary point occurs at the constraint boundary and (114) is the unique solution to (113). Now, consider the case where $\Sigma_x^i[m, m] + (\mu^i[m])^2 > 0$. The derivative of the objective function in (113) is given by

$$\frac{1}{2(\gamma^i[m])^2} \left(-\gamma^i[m] + \Sigma_x^i[m, m] + (\mu^i[m])^2 \right). \quad (115)$$

Since we are only interested in whether or not (115) is positive near 0, we drop the first term and inspect the limit as $\gamma^i[m] \rightarrow 0$:

$$\lim_{\gamma^i[m] \rightarrow 0} -\gamma^i[m] + \Sigma_x^i[m, m] + (\mu_j^i[m])^2 > 0. \quad (116)$$

This suggests that (115) is positive near the constraint boundary (in this regime), and so $\gamma^i[m] = 0$ cannot be a solution to (113) since this point is not even a local maximizer of $Q(\theta, \theta^t)$ in the neighborhood $\gamma^i[m] \in [0, \epsilon]$, $\epsilon > 0$. Therefore, when $\Sigma_x^i[m, m] + (\mu^i[m])^2 > 0$, (114) is the unique solution of (113).

Appendix H. Proof of Thm. 8

This proof is an extension of the proof shown in (Aharon et al., 2006b). Under the assumptions of Theorem 8, we can focus exclusively on recovering $\{D_j\}_{j=1}^J$ because, given $\{Y_j, D_j\}_{j=1}^J$, the sparse codes $\{X_j\}_{j=1}^J$ are unique (Donoho and Elad, 2003). To prove that $\{D_j\}_{j=1}^J$ is unique, we will show how $\{D_j\}_{j=1}^J$ can be recovered by construction.

The construction of $\{\hat{D}_j\}_{j=1}^J$ proceeds in three steps:

1. Divide the columns of Y_j into $R = \binom{M}{s}$ sets $\{G_j^1, \dots, G_j^R\}$ for all j , where $G_j^k = \{i : y_j^i \in \text{span}(D_j[:, \Upsilon^k])\}$ and Υ^k denotes the k 'th subset of size s of $[M]$.
2. Detect pairs $(G_j^{k_1}, G_j^{k_2})$ such that $|G_j^{k_1} \cap G_j^{k_2}| = 1$ for all j .
3. For each j , find the atom common to Υ^{k_1} and Υ^{k_2} . This atom is necessarily one of the atoms of D_j (Aharon et al., 2006b). Repeat for all pairs (k_1, k_2) .

We begin by describing how the data is clustered. Starting with modality j^* , we begin by testing every group of $s + 1$ data points from Y_{j^*} . The rank of this group of points will be s if and only if the points lie in the subspace spanned by a set of s columns from D_{j^*} (Aharon et al., 2006b). Once $\{G_{j^*}^k\}_{k=1}^R$ has been established, the remaining points in Y_{j^*} which have not been assigned to a set are combined with one of the groups $G_{j^*}^k$ based on the fact that the rank of the subspace spanned by the columns indexed by $G_{j^*}^k$ and an additional column, $y_{j^*}^i$, from Y_{j^*} is s if and only if $y_{j^*}^i \in \text{span}(D_{j^*}[:, \Upsilon_k])$. Finally, due to the nature of the data generation process, we know that $G_j^k = \{i : P[j, i] = 1 \text{ and } i \in G_{j^*}^k\}, \forall j$. Note that the construction of $G_{j^*}^k$ requires $s + 1$ data points from modality j^* , but we get G_j^k directly from $G_{j^*}^k$.

Next, we describe the process by which we detect pairs $(G_j^{k_1}, G_j^{k_2})$ such that $|\Upsilon^{k_1} \cap \Upsilon^{k_2}| = 1$. This can be done for each modality j independently. Namely, for each pair $(G_j^{k_1}, G_j^{k_2})$, we test the rank of the subspace spanned by the columns of Y_j indexed by $G_j^{k_1} \cup G_j^{k_2}$. The rank of this subspace will be $2s - 1$ if and only if the intersection of $\text{span}(G_j^{k_1})$ and $\text{span}(G_j^{k_2})$ has dimension 1. This process is guaranteed to produce every atom of D_j at least once (Aharon et al., 2006b).

Finally, we describe how to form \hat{D}_j . Given a pair $(G_j^{k_1}, G_j^{k_2})$ such that $|\Upsilon^{k_1} \cap \Upsilon^{k_2}| = 1$, we extract any s points from $G_j^{k_1}$ and any s points from $G_j^{k_2}$ and concatenate them into two matrices B^{k_1} and B^{k_2} , respectively. There exist vectors v^1 and v^2 such that both $B^{k_1}v^1$ and $B^{k_2}v^2$ are parallel to the atom of D_j of interest. We can now set up a system of equations given by

$$\underbrace{\begin{bmatrix} B^{k_1} & -B^{k_2} \end{bmatrix}}_B \underbrace{\begin{bmatrix} v^1 \\ v^2 \end{bmatrix}}_v = 0 \tag{117}$$

and find v , which is guaranteed to exist since $\text{rank}(B) = 2s - 1$ from the detection step. We can then extract v^1 from v and find one of the columns of D_j (up to scaling) using $B^{k_1}v^1$. This process can be repeated to find all M atoms of D_j (up to scale) (Aharon et al., 2006b).

The major difference between the proof given here and the one in (Aharon et al., 2006b) for the unimodal dictionary learning problem is that we require $s + 1$ data points per every s dimensional subspace for *one* of the modalities and only s data points per subspace for the rest of the modalities. The reason that we can use *less* samples stems from the special structure of the multimodal data generation process. In the end, we require $s + 1$ data points from modality j^* to complete the data clustering step and s data points from each of the $J - 1$ data modalities to complete the extraction step.

References

- M. Aharon, M. Elad, and A. Bruckstein. k -svd: An algorithm for designing overcomplete dictionaries for sparse representation. *IEEE Transactions on Signal Processing*, 54(11): 4311–4322, Nov 2006a. ISSN 1053-587X. doi: 10.1109/TSP.2006.881199.
- Michal Aharon, Michael Elad, and Alfred M Bruckstein. On the uniqueness of overcomplete dictionaries, and a practical way to retrieve them. *Linear algebra and its applications*, 416(1):48–67, 2006b.
- S Derin Babacan, Rafael Molina, and Aggelos K Katsaggelos. Variational bayesian super resolution. *IEEE Transactions on Image Processing*, 20(4):984–999, 2011.
- S. Bahrapour, N. M. Nasrabadi, A. Ray, and W. K. Jenkins. Multimodal task-driven dictionary learning for image classification. *IEEE Transactions on Image Processing*, 25(1):24–38, Jan 2016. ISSN 1057-7149.
- Dror Baron, Marco F Duarte, Michael B Wakin, Shriram Sarvotham, and Richard G Baraniuk. Distributed compressive sensing. *arXiv preprint arXiv:0901.3403*, 2009.

- Herbert Bay, Tinne Tuytelaars, and Luc Van Gool. Surf: Speeded up robust features. In *European conference on computer vision*, pages 404–417. Springer, 2006.
- James Bergstra and Yoshua Bengio. Random search for hyper-parameter optimization. *Journal of Machine Learning Research*, 13(Feb):281–305, 2012.
- James S Bergstra, Rémi Bardenet, Yoshua Bengio, and Balázs Kégl. Algorithms for hyper-parameter optimization. In *Advances in Neural Information Processing Systems*, pages 2546–2554, 2011.
- Aurélie Boisbunon. The class of multivariate spherically symmetric distributions. 2012.
- Damian Borth, Rongrong Ji, Tao Chen, Thomas Breuel, and Shih-Fu Chang. Large-scale visual sentiment ontology and detectors using adjective noun pairs. In *Proceedings of the 21st ACM international conference on Multimedia*, pages 223–232. ACM, 2013.
- Stephen Boyd and Lieven Vandenberghe. *Convex optimization*. Cambridge university press, 2004.
- James V. Burke. *Undergraduate Nonlinear Continuous Optimization*.
- Juan C Caicedo and Fabio A González. Multimodal fusion for image retrieval using matrix factorization. In *Proceedings of the 2nd ACM international conference on multimedia retrieval*, page 56. ACM, 2012.
- Emmanuel J Candes, Michael B Wakin, and Stephen P Boyd. Enhancing sparsity by reweighted ℓ_1 minimization. *Journal of Fourier analysis and applications*, 14(5-6):877–905, 2008.
- Miriam Cha, Youngjune Gwon, and HT Kung. Multimodal sparse representation learning and applications. *arXiv preprint arXiv:1511.06238*, 2015.
- Gabriella Csurka, Christopher Dance, Lixin Fan, Jutta Willamowski, and Cédric Bray. Visual categorization with bags of keypoints. In *Workshop on statistical learning in computer vision, ECCV*, volume 1, pages 1–2. Prague, 2004.
- Yacong Ding and Bhaskar D Rao. Joint dictionary learning and recovery algorithms in a jointly sparse framework. In *2015 49th Asilomar Conference on Signals, Systems and Computers*, pages 1482–1486. IEEE, 2015.
- D. L. Donoho, M. Elad, and V. N. Temlyakov. Stable recovery of sparse overcomplete representations in the presence of noise. *IEEE Transactions on Information Theory*, 52(1):6–18, Jan 2006. ISSN 0018-9448. doi: 10.1109/TIT.2005.860430.
- David L Donoho and Michael Elad. Optimally sparse representation in general (nonorthogonal) dictionaries via ℓ_1 minimization. *Proceedings of the National Academy of Sciences*, 100(5):2197–2202, 2003.
- Torbjørn Eltoft, Taesu Kim, and Te-Won Lee. On the multivariate laplace distribution. *IEEE Signal Processing Letters*, 13(5):300–303, 2006.

- I. Fedorov, R. Giri, B. D. Rao, and T. Q. Nguyen. Robust bayesian method for simultaneous block sparse signal recovery with applications to face recognition. In *2016 IEEE International Conference on Image Processing (ICIP)*, pages 3872–3876, Sept 2016. doi: 10.1109/ICIP.2016.7533085.
- I. Fedorov, B. D. Rao, and T. Q. Nguyen. Multimodal sparse bayesian dictionary learning applied to multimodal data classification. In *2017 IEEE International Conference on Acoustics, Speech and Signal Processing (ICASSP)*, pages 2237–2241, March 2017. doi: 10.1109/ICASSP.2017.7952554.
- Igor Fedorov, Alican Nalci, Ritwik Giri, Bhaskar D. Rao, Truong Q. Nguyen, and Harinath Garudadri. A unified framework for sparse non-negative least squares using multiplicative updates and the non-negative matrix factorization problem. *Signal Processing*, 146:79 – 91, 2018. ISSN 0165-1684. doi: <https://doi.org/10.1016/j.sigpro.2018.01.001>. URL <http://www.sciencedirect.com/science/article/pii/S0165168418300033>.
- James E Gentle. *Matrix algebra: theory, computations, and applications in statistics*. Springer Science & Business Media, 2007.
- R. Giri and B. Rao. Type I and Type II Bayesian Methods for Sparse Signal Recovery Using Scale Mixtures. *IEEE Transactions on Signal Processing*, 64(13):3418–3428, July 2016. ISSN 1053-587X. doi: 10.1109/TSP.2016.2546231.
- Mark Girolami. A variational method for learning sparse and overcomplete representations. *Neural computation*, 13(11):2517–2532, 2001.
- Hendra Gunawan, Oki Neswan, and Wono Setya-Budhi. A formula for angles between subspaces of inner product spaces. *Contributions to Algebra and Geometry*, 46(2):311–320, 2005.
- Asela Gunawardana and William Byrne. Convergence theorems for generalized alternating minimization procedures. *Journal of Machine Learning Research*, 6(Dec):2049–2073, 2005.
- Youngjune Gwon, William Campbell, Kevin Brady, Douglas Sturim, Miriam Cha, and H.T. Kung. Multimodal sparse coding for event detection. *NIPS MMML*, 2015.
- Rodolphe Jenatton, Julien Mairal, Guillaume Obozinski, and Francis R Bach. Proximal methods for sparse hierarchical dictionary learning. In *ICML*, number 2010, pages 487–494. Citeseer, 2010.
- Rodolphe Jenatton, Jean-Yves Audibert, and Francis Bach. Structured variable selection with sparsity-inducing norms. *Journal of Machine Learning Research*, 12(Oct):2777–2824, 2011.
- Shihao Ji, David Dunson, and Lawrence Carin. Multitask compressive sensing. *IEEE Transactions on Signal Processing*, 57(1):92–106, 2009.

- Zhuolin Jiang, Zhe Lin, and Larry S Davis. Label consistent k-svd: Learning a discriminative dictionary for recognition. *Pattern Analysis and Machine Intelligence, IEEE Transactions on*, 35(11):2651–2664, 2013.
- Seyoung Kim and Eric P Xing. Tree-guided group lasso for multi-task regression with structured sparsity. 2010.
- Igor Kviatkovsky, Moshe Gabel, Ehud Rivlin, and Ilan Shimshoni. On the equivalence of the lc-ksvd and the d-ksvd algorithms. *IEEE transactions on pattern analysis and machine intelligence*, 39(2):411–416, 2017.
- David JC MacKay. Bayesian interpolation. *Neural computation*, 4(3):415–447, 1992.
- David JC MacKay. Hyperparameters: optimize, or integrate out? *Fundamental theories of physics*, 62:43–60, 1996.
- Julien Mairal, Francis Bach, Jean Ponce, and Guillermo Sapiro. Online dictionary learning for sparse coding. In *Proceedings of the 26th annual international conference on machine learning*, pages 689–696. ACM, 2009.
- Julien Mairal, Francis Bach, and Jean Ponce. Task-driven dictionary learning. *IEEE Transactions on Pattern Analysis and Machine Intelligence*, 34(4):791–804, 2012.
- Yosra Marnissi, Yuling Zheng, Emilie Chouzenoux, and Jean-Christophe Pesquet. A variational bayesian approach for image restoration. application to image deblurring with poisson-gaussian noise. *IEEE Transactions on Computational Imaging*, 2017.
- Alican Nalci, Igor Fedorov, Maher Al-Shoukairi, Thomas T Liu, and Bhaskar D Rao. Rectified gaussian scale mixtures and the sparse non-negative least squares problem. *arXiv preprint arXiv:1601.06207*, 2016.
- Radford M Neal and Geoffrey E Hinton. A view of the em algorithm that justifies incremental, sparse, and other variants. In *Learning in graphical models*, pages 355–368. Springer, 1998.
- Jason Allan Palmer. Variational and scale mixture representations of non-gaussian densities for estimation in the bayesian linear model: Sparse coding, independent component analysis, and minimum entropy segmentation. 2006.
- Neal Parikh, Stephen Boyd, et al. Proximal algorithms. *Foundations and Trends® in Optimization*, 1(3):127–239, 2014.
- Yagyensh Chandra Pati, Ramin Rezaifar, and PS Krishnaprasad. Orthogonal matching pursuit: Recursive function approximation with applications to wavelet decomposition. In *Signals, Systems and Computers, 1993. 1993 Conference Record of The Twenty-Seventh Asilomar Conference on*, pages 40–44. IEEE, 1993.
- James R Schott. *Matrix analysis for statistics*. John Wiley & Sons, 2016.

- S. Shekhar, V. M. Patel, N. M. Nasrabadi, and R. Chellappa. Joint sparse representation for robust multimodal biometrics recognition. *IEEE Transactions on Pattern Analysis and Machine Intelligence*, 36(1):113–126, Jan 2014. ISSN 0162-8828. doi: 10.1109/TPAMI.2013.109.
- Michael E Tipping. Sparse bayesian learning and the relevance vector machine. *The journal of machine learning research*, 1:211–244, 2001.
- David P Wipf and Bhaskar D Rao. Sparse bayesian learning for basis selection. *Signal Processing, IEEE Transactions on*, 52(8):2153–2164, 2004.
- David P Wipf and Bhaskar D Rao. An empirical bayesian strategy for solving the simultaneous sparse approximation problem. *Signal Processing, IEEE Transactions on*, 55(7):3704–3716, 2007.
- David P Wipf, Bhaskar D Rao, and Srikantan Nagarajan. Latent variable bayesian models for promoting sparsity. *Information Theory, IEEE Transactions on*, 57(9):6236–6255, 2011.
- CF Jeff Wu. On the convergence properties of the em algorithm. *The Annals of statistics*, pages 95–103, 1983.
- Jianchao Yang, John Wright, Thomas S Huang, and Yi Ma. Image super-resolution via sparse representation. *Image Processing, IEEE Transactions on*, 19(11):2861–2873, 2010.
- Linxiao Yang, Jun Fang, and Hongbin Li. Sparse bayesian dictionary learning with a gaussian hierarchical model. In *2016 IEEE International Conference on Acoustics, Speech and Signal Processing (ICASSP)*, pages 2564–2568. IEEE, 2016.
- Ganchi Zhang and Nick Kingsbury. Fast l0-based image deconvolution with variational bayesian inference and majorization-minimization. In *Global Conference on Signal and Information Processing (GlobalSIP), 2013 IEEE*, pages 1081–1084. IEEE, 2013.
- Ganchi Zhang, Timothy D Roberts, and Nick Kingsbury. Image deconvolution using tree-structured bayesian group sparse modeling. In *Image Processing (ICIP), 2014 IEEE International Conference on*, pages 4537–4541. IEEE, 2014.
- Qiang Zhang and Baoxin Li. Discriminative k-svd for dictionary learning in face recognition. In *Computer Vision and Pattern Recognition (CVPR), 2010 IEEE Conference on*, pages 2691–2698. IEEE, 2010.
- Z. Zhang and B. D. Rao. Sparse signal recovery with temporally correlated source vectors using sparse bayesian learning. *IEEE Journal of Selected Topics in Signal Processing*, 5(5):912–926, Sept 2011. ISSN 1932-4553. doi: 10.1109/JSTSP.2011.2159773.
- Peng Zhao, Guilherme Rocha, and Bin Yu. The composite absolute penalties family for grouped and hierarchical variable selection. *The Annals of Statistics*, pages 3468–3497, 2009.

Renbo Zhao and Vincent YF Tan. A unified convergence analysis of the multiplicative update algorithm for nonnegative matrix factorization. *arXiv preprint arXiv:1609.00951*, 2016.